



Cite this: *Soft Matter*, 2022, 18, 6487

Received 3rd June 2022,  
Accepted 7th August 2022

DOI: 10.1039/d2sm00733a

[rsc.li/soft-matter-journal](http://rsc.li/soft-matter-journal)

## Materials development in stretchable iontronics

Jae-Man Park,<sup>†</sup><sup>a</sup> Sungsoo Lim<sup>ID</sup><sup>†</sup><sup>a</sup> and Jeong-Yun Sun<sup>ID</sup><sup>\*</sup><sup>ab</sup>

Stretchable iontronics have recently been developed as an ideal interface to promote the interaction between humans and devices. Since the materials that use ions as charge carriers are typically transparent and stretchable, they have been used to fabricate devices with diverse functions with intrinsic transparency and stretchability. With the development of device design, material design has also been investigated to mitigate the issues associated with ionic materials, such as their weak mechanical properties, poor electrical properties, or poor environmental stabilities. In this review, we describe the recent progress on the design of materials in stretchable iontronics. By classifying stretchable ionic materials into three types of components (ionic conductors, ionic semiconductors, and ionic insulators), the issues each component has and the strategies to solve them are introduced, specifically in terms of molecular interactions. We then discuss the existing hurdles and challenges to be handled and shine light on the possibilities and opportunities from the insight of molecular interactions.

### 1. Introduction

The engineered devices that are currently being used by humans have been developed to be thinner, lighter, and more flexible.<sup>1–3</sup> Insight into the conformability of humans to use devices harnesses the concept of wearable or epidermal electronics;<sup>4</sup> therefore, researchers over the past few decades have demonstrated diverse electronic devices with stretchable

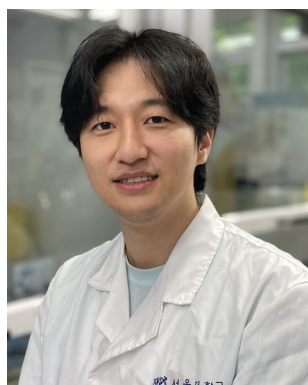
forms, including sensors,<sup>5–7</sup> actuators,<sup>8,9</sup> transistors,<sup>10–13</sup> and displays.<sup>14–18</sup> Unfortunately, as these electronic devices are often made of rigid materials, researchers have introduced geometric designs, composites with stretchable substrates, or molecular engineering<sup>19–21</sup> for the stretchability. Nevertheless, those devices have suffered from reduced performances in the stretched state, as well as limited stretchability.

The concept of stretchable iontronics, where ions can be used as charge carriers without electrochemical reactions in a specific design, was developed in 2013.<sup>22</sup> Since ionically conductive materials are typically highly transparent and stretchable (e.g., ionic-salt-dissolved hydrogels), numerous types of conventional electronic devices have been transformed into intrinsically stretchable and transparent ionic devices, including loudspeakers,<sup>22</sup> sensors, and touch pads,<sup>23–25</sup> displays,<sup>26–29</sup> energy

<sup>a</sup> Department of Materials Science and Engineering, Seoul National University, Seoul 08826, Republic of Korea. E-mail: [jysun@snu.ac.kr](mailto:jysun@snu.ac.kr), [parkdora2@snu.ac.kr](mailto:parkdora2@snu.ac.kr), [limss0719@snu.ac.kr](mailto:limss0719@snu.ac.kr)

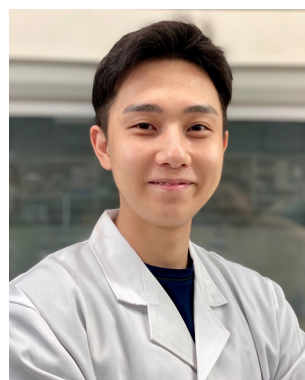
<sup>b</sup> Research Institute of Advanced Materials (RIAM), Seoul National University, Seoul 08826, Republic of Korea

† These authors contributed equally to this paper.



**Jae-Man Park**

*Jae-Man Park received his B.S. (2017) from Department of Materials Science and Engineering at the Seoul National University, Republic of Korea. He is currently an integrated Ph.D. candidate in materials science and engineering at the Seoul National University under the supervision of Prof. Jeong-Yun Sun. He is interested in designing molecular structures and interactions in polymeric materials.*



**Sungsoo Lim**

*Sungsoo Lim received his B.S. (2016) from Department of Materials Science and Engineering at the Seoul National University, Republic of Korea. He is currently an integrated Ph.D. candidate in materials science and engineering at the Seoul National University under the supervision of Prof. Jeong-Yun Sun. He is currently working on the development and synthesis of ionic materials.*

sources and generators,<sup>30–32</sup> actuators,<sup>22,33,34</sup> electro-adhesives,<sup>35,36</sup> and computational elements<sup>37,38</sup> (Fig. 1).

Along with these developments in the device design, the design of materials has also been investigated. To design and fabricate stretchable ionic devices, stretchable ionic components are needed, where each component (ionic conductors, ionic semiconductors, and ionic insulators) performs different functions under stretch. Therefore, the preparation of proper materials for each ionic component must precede, material selection and combination, while considering the structures and morphologies of polymer networks, or the micro- and nanophases. In these processes, it is crucial to consider molecular interactions for tuning and understanding the properties of materials.

Many researchers have reported comprehensive review papers summarizing recent progress on the device design of stretchable iontronics,<sup>39–41</sup> nonetheless, there have been few papers focussing on material development in stretchable iontronics. In this review, we provide a comprehensive summary of the progress on the material design in stretchable iontronics. We first classify the forms of stretchable ionic functional materials, briefly explain the theory of mixing and types of molecular interactions, and introduce representative studies that have attempted to improve the properties of ionic materials. In particular, we aim to highlight the studies where insights into molecular interactions have led to significant improvements in the materials. Lastly, we discuss the current limitations and challenges with stretchable ionic materials, and then suggest directions for future studies on the design of stretchable iontronic materials.

## 2. Design of stretchable ionic materials

### 2.1. Types and forms of stretchable ionic components

Stretchable iontronics mainly consist of three components; (i) Stretchable ionic conductors (SICs), where the stretchable



Jeong-Yun Sun

University. After his Post-Doc., he came back to SNU and served as an assistant professor for 4 years. His research focuses on developing ionic materials and devices.

*Jeong-Yun Sun is currently an associate professor in the Department of Materials Science and Engineering at Seoul National University (SNU), Republic of Korea. He got his B.S. (2005), M.S. (2007) and Ph.D. (2012) in Materials Science and Engineering at Seoul National University. After getting Ph.D. (2012), he started to work as a postdoctoral fellow in School of Engineering and Applied Sciences at Harvard*

materials contain ions and solvate them, therefore they act as an electrolyte (Fig. 2a). (ii) Stretchable ionic semiconductors (SISs), where the stretchable materials contain an immobile specific charge and a mobile opposite charge, therefore they have ion selectivity (Fig. 2b). (iii) stretchable ionic insulators (SII), where the stretchable materials prevent ions from dissociation, therefore they act as a dielectric (Fig. 2c).

Since the SICs should dissociate ions, they are composed of hydrophilic and polar materials. Hydrogels are the representative materials in this case. The hydrogels consist of hydrophilic polymer networks that are swollen by water, thus allowing the ionic salts to be readily dissolved and hydrated in the hydrogels. As the hydrophilic network is plasticized by a large amount of water, the hydrogels are mechanically soft, highly stretchable, and transparent because of their amorphous structures. Similarly, when the polymer networks are swollen by organic solvents or ionic liquids (ILs), they are, respectively, called organogels or ionogels. When the organogels are made up of polar materials, they can hydrate ions, while the ionogels have mobile liquid ions, they both exhibit electrical behaviours similar to those of hydrogels.

The SISs should immobilize one type of ion and mobilize the opposite type of ion. Polymer networks containing positive or negative charges, namely, polyelectrolytes, can be used as ionic semiconductors. As the charged polymers are often mechanically rigid, they need plasticizers, such as water, solvents, or additional material engineering.

The SII should prevent ions from dissociation, so they are composed of hydrophobic and nonpolar materials. To achieve softness and stretchability, the SII would be designed with nonpolar polymer networks. When the polymer networks are rigid, they need nonpolar organic solvents as plasticizers. In some cases, molecular additives are required to tune the dielectric and mechanical properties.

All the three above-mentioned above are mostly mixtures of diverse materials. In order to mix different materials to form one desired material, it is important to consider the interactions between the materials. Functional groups in polymer networks, various types of ions, and molecules such as water, liquids, or particles interact in various delicate ways (Fig. 2d). Understanding their interactions is an essential aspect of material design for stretchable iontronics.

### 2.2. Intermolecular interactions in material design

When two or more materials are mixed, an interaction occurs. In terms of thermodynamics, the mixing phenomenon is explained by energetic and entropic preference.<sup>42,43</sup> The Gibbs free energy of mixing is  $\Delta G_{\text{mix}} = \Delta H_{\text{mix}} - T\Delta S_{\text{mix}}$ , where  $\Delta H_{\text{mix}}$  is the mixing enthalpy,  $\Delta S_{\text{mix}}$  is the mixing entropy, and  $T$  is temperature. Since  $\Delta S_{\text{mix}}$  is always positive in mixing, the determining factor of mixing is the value of  $\Delta H_{\text{mix}}$ . As an example, when component A and component B are mixed, the components overcome their respective noncovalent dissociation energies,  $\Delta H_A$  and  $\Delta H_B$  (Fig. 3a). Then, they are stabilized by the formation of interactions between them. The mixing enthalpy is  $\Delta H_{\text{mix}} = kTN\phi\chi$ , where  $k$  is the Boltzmann

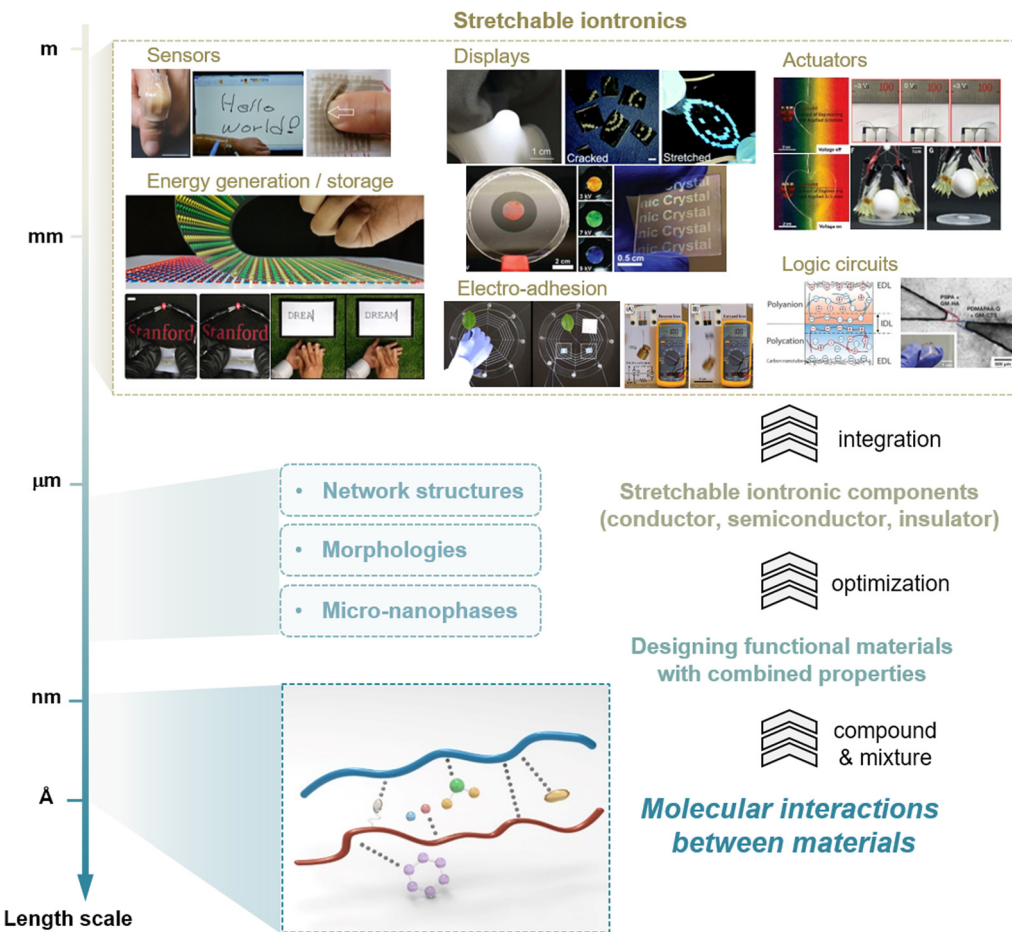


**Fig. 1** Materials science in stretchable iontronics. Examples of stretchable iontronic devices, including recognition of mechanical stimuli, luminescent or reflective displays, electroactive actuators, energy sources or energy generator, electro-adhesions, and ionic circuit elements. The components of stretchable iontronics are designed to be functional while having intrinsic stretchability. The engineering of the materials has originated from the consideration of molecular interactions. The materials design for stretchable iontronics, therefore, starts from the understanding of molecular interactions between materials. Reproduced with permission from ref. 22, 24, 25, 26, 29, 34, 35 and 37. Copyright 2013, 2016, 2018, and 2020, AAAS. Reproduced with permission from ref. 23, 28, 36 and 38. Copyright 2014, 2018, and 2020, Wiley-VCH. Reproduced with permission from ref. 30 and 31–33. Copyright 2016, 2017, 2018, and 2019, Springer Nature. Reproduced with permission from ref. 27. Copyright 2018, The Royal Society of Chemistry.

constant,  $N$  is the number of components,  $\phi$  is the fraction of a component and  $\chi$  is the interaction parameter. The interaction parameter  $\chi$  is proportional to the difference in the solubility parameter  $\delta$  of each component, which is written as  $\chi = V(\delta_A - \delta_B)^2/kT$ , where  $V$  is the volume of a component. In addition,  $\delta$  is relative to the dissociation enthalpy, which is written as  $\delta = [(\Delta H - kT)/V]^{1/2}$ . Therefore, when the two components have similar values of  $\Delta H$ , in other words, when  $\chi$  is low, the components can be more miscible to facilitate mixing. In contrast, when the two components have dissimilar values of  $\Delta H$  or high  $\chi$ , their phases are separated.

In nature, diverse noncovalent molecular interactions exist, including van der Waals interaction, dipole–dipole interaction, aromatic pi–pi interaction, hydrogen bonding, ion–dipole interaction, and ionic interaction (Fig. 3b). The  $\Delta H$  values of these interactions are distributed between thermal energy at room temperature  $k_B T$  and covalent dissociation energies.<sup>44–53</sup> We present representative molecular forms of diverse interactions

in polymer engineering, ranging from induced dipole interactions between little-polarized groups (van der Waals, *e.g.*  $-\text{CH}_x$  moieties), dipole interactions between slightly polarized groups (*e.g.*  $-\text{CH}_x$ ,  $-\text{CF}_x$ , or  $-\text{COO}^-$  moieties), pi–pi interactions and quadrupole pi–pi interactions between aromatic groups, to various types of hydrogen bonding (H-bonding, *e.g.*,  $-\text{CONH}^-$ , *etc.*), ion–dipole interactions of cations with negative dipole groups or anions with positive dipole groups, and ionic interactions (*e.g.* strong sulfonate and ammonium ions, or weak carboxylic and imidazolium ions) (Fig. 3c). Diverse moieties, including those stated above, have previously been utilized in the design of polymers, ions, molecules, or particle surfaces, to form miscible or multi-phase mixtures.

In the next section, we introduce the material development of each ionic component by focusing on the strategies for material engineering with molecular interactions. We briefly explain the characteristics and requirements of each component, and we discuss the trends and developments of stretchable

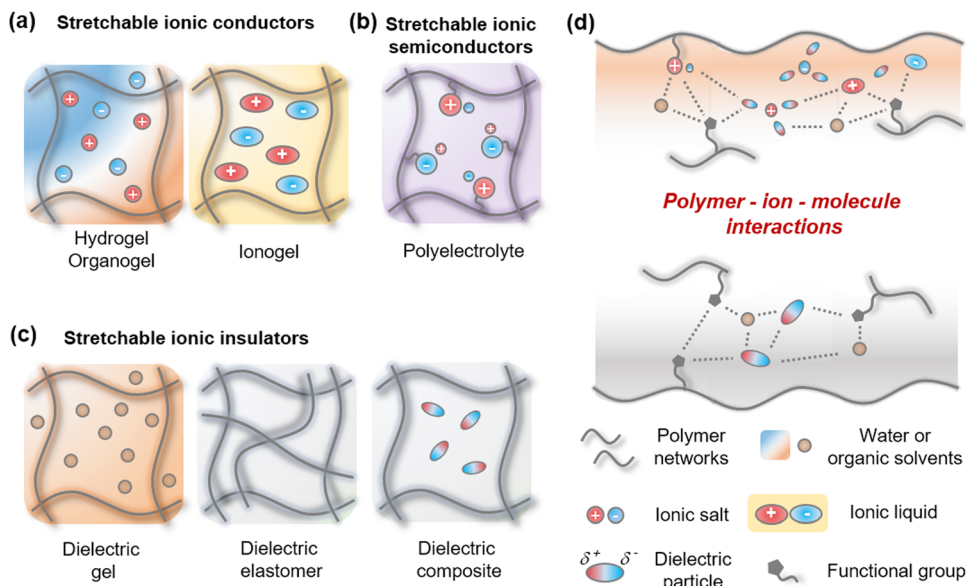


**Fig. 2** Types and forms of stretchable iontronic components. Stretchable iontronics mainly consists of three components: (a) stretchable ionic conductors (SICs), (b) stretchable ionic semiconductors (SISs), and (c) stretchable ionic insulators (SII). They are composed of polymer networks, solvents, ions, molecules, or particles. (d) Diverse interactions between polymers, ions, molecules, or particles exist to form stretchable ionic components.

iontronic materials, particularly from the perspective of molecular interactions whenever possible.

### 3. Stretchable ionic conductors (SICs)

SICs are the most important components for stretchable iontronics. The SICs have two requirements in terms of their functionality; (i) stretchable networks for their shape retention, and (ii) solvated ions for ionic conductivity. Therefore, the interactions of polymers or solvents with ions should be favourable. In other words, low  $\chi$  values between them are preferred.

#### 3.1. Types of SICs

Researchers have developed four types of SICs: hydrogels, organogels, ionogels, and ionoelastomers (Fig. 4a and b). Hydrogels are water-swollen hydrophilic networks, and organogels are organic-solvent swollen networks. Their polar environment enables the solvation of ionic salts. Ionogels are IL-containing polymer networks, so ILs act as both plasticizers and electrolytes. Ionoelastomers are liquid-free and ionic conductive polymeric networks, where the ionic salts are dissolved without solvents or the ions are bound to polymer networks. Each type has distinct characteristics. Briefly, the gel materials have high ionic conductivity, but have low stabilities. Hydrogels are highly stretchable and biocompatible, organogels are less volatile than hydrogels,<sup>28</sup> and ionogels are non-volatile.<sup>54</sup> Meanwhile, although, the elastomers exhibit high stabilities, such as no liquid leakage, a wide electrochemical window, and non-volatility, they suffer from low ionic conductivity. In the following section, we introduce the development of each type of material more specifically.

#### 3.2. Hydrogel-based SICs

Unlike electronic conductors, an ionic conductor can generate electrochemical reactions when it is associated with an electronic power source. Since the chemical reaction changes the chemical state of a material, the ionic conductors require specific designs to prevent electrochemical reactions.

Suo *et al.* presented a device design wherein a dielectric layer was placed between two electrolyte layers, and the electrolytes were connected to electrodes.<sup>22</sup> Due to the very small value of capacitance compared to the capacitance in electric double layers, the interfaces between the electrolyte and the dielectric took up most of the applied voltages (Fig. 5a). Therefore, the devices are able to operate at high voltages above 10 kilovolts and high frequencies above 10 kilohertz. When the voltage is applied, no chemical reaction occurs, as the charge is accumulated at the surface of the dielectric, thus causing electrostatic actuation. The researchers chose hydrogels for the ionic conductors because the hydrogels are highly soft, stretchable, and transparent. They demonstrated soft and transparent actuators and loudspeakers (Fig. 5b). Although the hydrogel-based iontronic devices exhibit relatively higher resistivity than electronic conductors, their change in resistivity under stretch is lower than that of all existing electronic conductors, thus representing a significant advancement in the design of stretchable devices (Fig. 5c).

In the above study, researchers used hydrogels as SICs since the hydrogels are highly stretchable, transparent, biocompatible, and easy to fabricate. The hydrogels are made up of  $\sim 90\%$  of water and cross-linked polyacrylamide (PAAm) networks, and sodium chloride salts. Water highly hydrates the ionic salts, and the PAAm interacts with water by strong hydrogen bonding, as a result, the ionically conductive hydrogels are formed. Numerous hydrogel-based papers, describing designs with

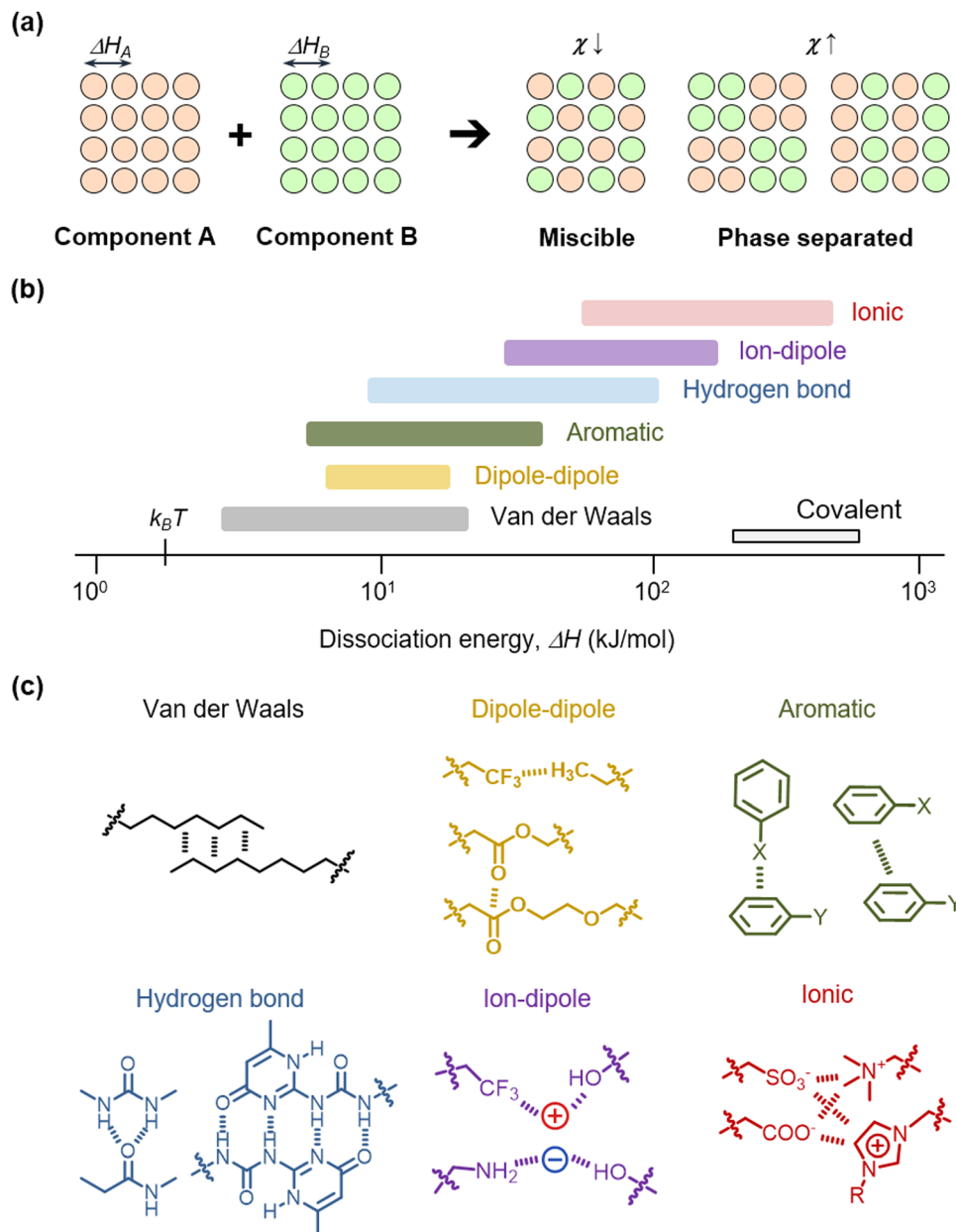


**Fig. 3** Intermolecular interactions for materials design. (a) When two components are mixed, the interaction parameter  $\chi$  is a determinant factor for their miscibility. (b) A scale of the dissociation energy of diverse molecular interactions. The  $k_B T$  is thermal energy at room temperature. (c) Representative molecular moieties for different intermolecular interactions.

water-soluble polymers and ionic salts, have been reported as soft SICs.<sup>39,58,59</sup>

Unfortunately, water has inherently high vapor pressure, which causes the hydrogel-based ionic devices to suffer from operational stability because the evaporation of water makes the gel brittle and non-conductive. One study reported that high concentrations of deliquescent ionic salts (e.g., lithium chloride) delayed the evaporation of water in hydrogels,<sup>60</sup> although there was still 60% water loss within 2 days.

P.S. Lee *et al.* reported self-healable and thermally stable hydrogel-based SICs.<sup>57</sup> In that study, the researchers took a three-pronged holistic approach: (i) add glycerol as an additive

to lower the vapour pressure, (ii) adopt polyelectrolyte networks (wherein ionic charges are attached to polymers) to prevent phase separation between ionic salts and hydrogels during temperature changes, and (iii) copolymerize polyelectrolyte monomers of 3-sulfopropyl methacrylate potassium salt (SPMA) with hydrophobic monomers of methyl methacrylate (MMA) to increase physical crosslinking and entanglements to enhance the mechanical properties (Fig. 5d). The designed hydrogels are self-supported, mechanically robust, self-healable, and thermally stable, and they demonstrated a stable operation of dielectric elastomer actuators (DEAs) with the gels under 100 °C for 420 min (Fig. 5e).

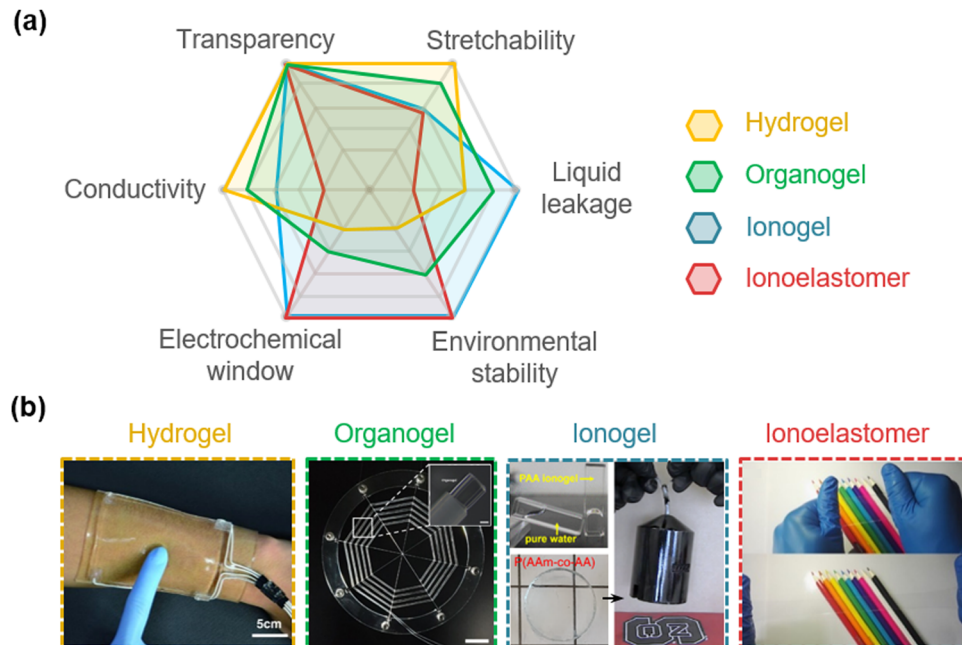


Fig. 4 Types of SICs. (a) Characteristics of different SICs. (b) Photograph images of different SICs. Reproduced with permission from ref. 54. Copyright 2014, The American Chemical Society. Reproduced with permission from ref. 24 and 35. Copyright 2016, and 2020, AAAS. Reproduced with permission from ref. 55 and 56. Copyright 2018, and 2022, Springer Nature.

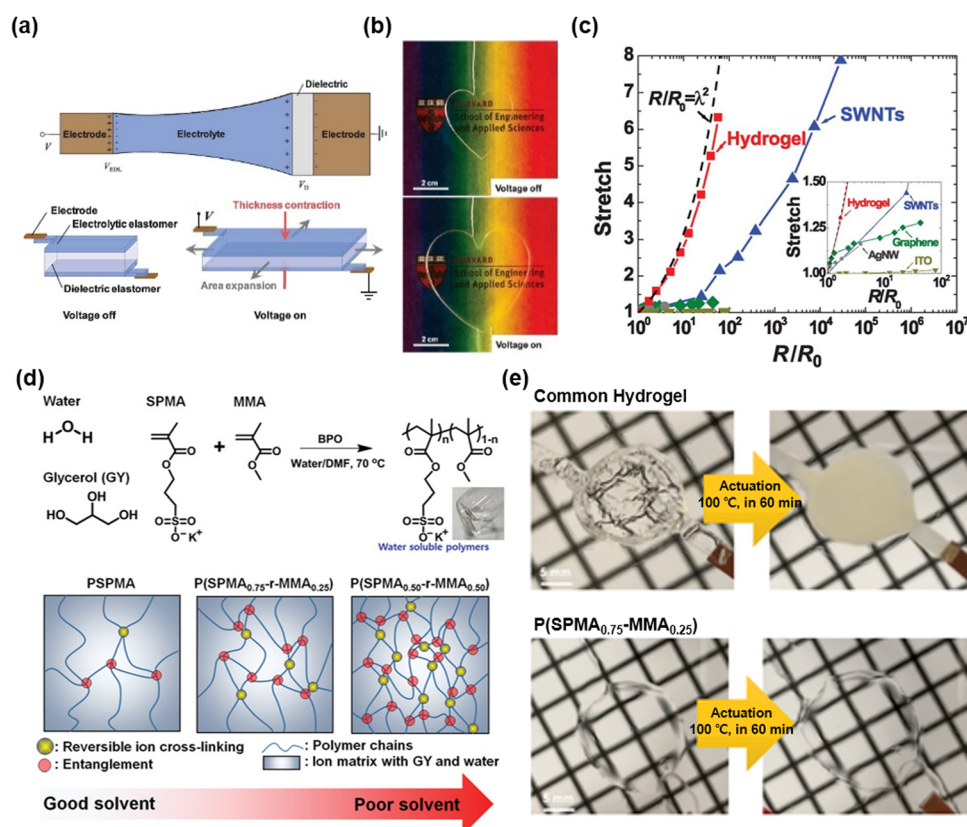


Fig. 5 Hydrogel-based SICs. (a) The device structure of hydrogel-based stretchable ionics. (b) Photograph images of transparent, stretchable electroactive hydrogels. (c) Resistance changes in hydrogels by stretch compared to the electronic conductors. Reproduced with permission from ref. 22. Copyright 2013, AAAS. (d) Materials for stable hydrophobic polyelectrolyte SICs, and schematics of hydrophobic monomer (MMA) effect on chain entanglement. (e) Photographs of the operation of dielectric elastomer actuator (DEA) based on common hydrogel (top) and the designed materials (bottom) under 100 °C for 60 min. Reproduced with permission from ref. 57. Copyright 2019, Wiley-VCH.

### 3.3. Organogel-based SICs

In response to the volatility issue of hydrogels, some researchers have attempted to design low-volatile organic solvent-based organogel ionic conductors. For example, Ding *et al.* reported propylene carbonate (PC)-based organogel ionic conductors.<sup>61</sup> The PC has been widely used as a solvent electrolyte in battery design.<sup>62</sup> The organogels consisted of an ionic salt of lithium bis(trifluoromethanesulfonyl)imide ( $\text{Li}^+\text{TFSI}^-$ ), PC solvent, and poly(4-acryloylmorpholine) (PACMO) networks. PC hydrates the  $\text{Li}^+\text{TFSI}^-$  salts, and the liquid electrolyte interacts with the hydrophilic PACMO networks by dipole interactions (Fig. 6a). The designed organogels are highly stretchable, transparent, ambient stable, and ionically conductive even at  $-20^\circ\text{C}$  (Fig. 6b and c). More recently, Sun *et al.* reported ethylene glycol (EG)-based organogel ionic conductors,<sup>35</sup> where the EG is a low-volatile solvent that enables the construction of diverse functional organogels with PAAm networks<sup>28,63</sup> (Fig. 6d). The researchers fabricated stretchable threads based on the organogel ionic conductors encapsulated with surface-fluorinated silicon elastomers. The applied voltage through the thread-induced electrostatic forces, and the researchers utilized this phenomenon to demonstrate artificial spiderwebs.

Furthermore, researchers have tried to develop organohydrogels as SICs, which are a hybrid form of hydrogels and organogels. The organohydrogels are composed of water and diverse organic solvents. Examples of the used hybrid solvent systems are glycerol/water,<sup>64–68</sup> dimethyl sulfoxide (DMSO)/water,<sup>69,70</sup> EG/water,<sup>71</sup> and 1,3-butandiol/water.<sup>72</sup> The utilization of organohydrogels as SICs exhibited hydrogel-like electrical

properties while they overcome the limitation of hydrogel-based SICs, such as being operative at subzero temperatures and stable long-term operation and storage under ambient conditions.

### 3.4. IL-based SICs (IL-SICs)

For the formation of SICs, solvents are needed to solvate ionic salts. However, solvents have vapor pressure, which leads to stability issues. Ionic liquids (ILs) are a unique class of materials, they themselves are in the liquid states, and they have a wide electrochemical window and negligible vapor pressure, due to the Coulombic pairs of bulky ions.<sup>73</sup> Therefore, researchers have investigated fabricating IL-based SICs.

IL-based SICs (IL-SICs) are composed of polymers and ILs. To combine polymers with ILs, it is important to find appropriate interactions between the functional groups of polymers and ILs, as these interactions determine their compatibility. The polymers can be roughly classified as polymer-based type<sup>52,74–88</sup> and monomer-based type,<sup>89–109</sup> and the ILs are composed of diverse pairs of the cationic and the anionic units (Fig. 7a and b). The negative dipoles could interact with the cations, whereas the positive dipoles could interact with the anions. By considering the dipole moments and hydrophilicity of polymers and ILs, we can expect the miscibility of candidates and fabricate on-demand IL-SICs.

Wang *et al.* reported poly(vinylidene fluoride-*co*-hexafluoropropylene) (PVDF-HFP) based self-healable transparent SICs.<sup>52</sup> Unlike conventional PVDF-HFP (HFP ratio of  $\sim 10\%$ ), they chose the PVDF-HFP with a high ratio of the HFP group

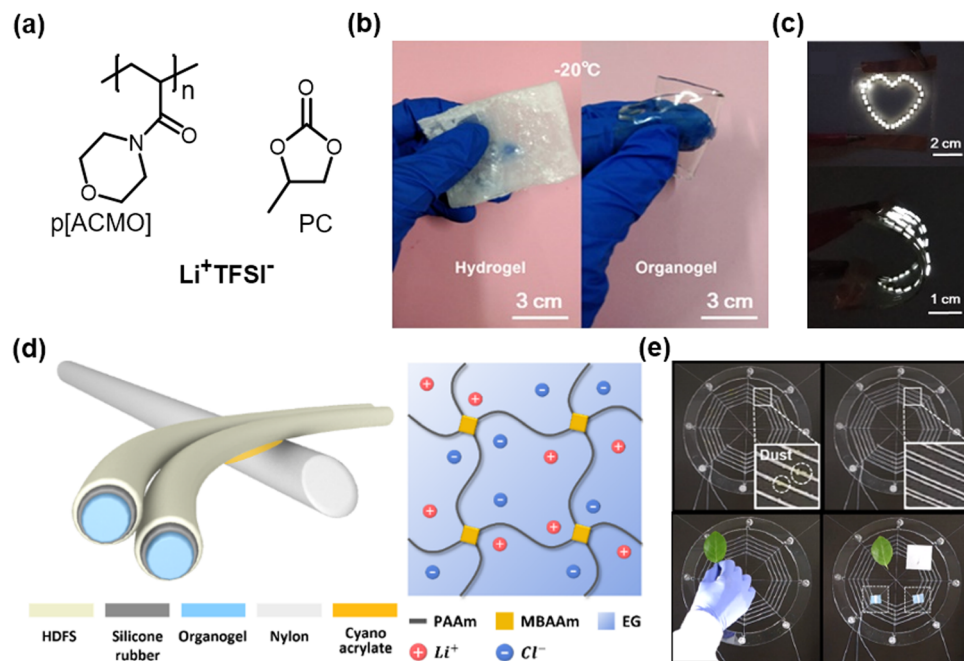


**Fig. 6** Organogel-based SICs. (a) One example of organogel-based ionic conductors. (b) The organogel ionic conductor is mechanically conformable at  $-20^\circ\text{C}$ . (c) The organogel ionic conductor as a stretchable electrode. Reproduced with permission from ref. 61. Copyright 2019, The American Chemical Society. (d) Another example of an organogel-based ionic conductor and its components. (e) Demonstration of artificial spiderwebs. Reproduced with permission from ref. 35. Copyright 2020, AAAS.

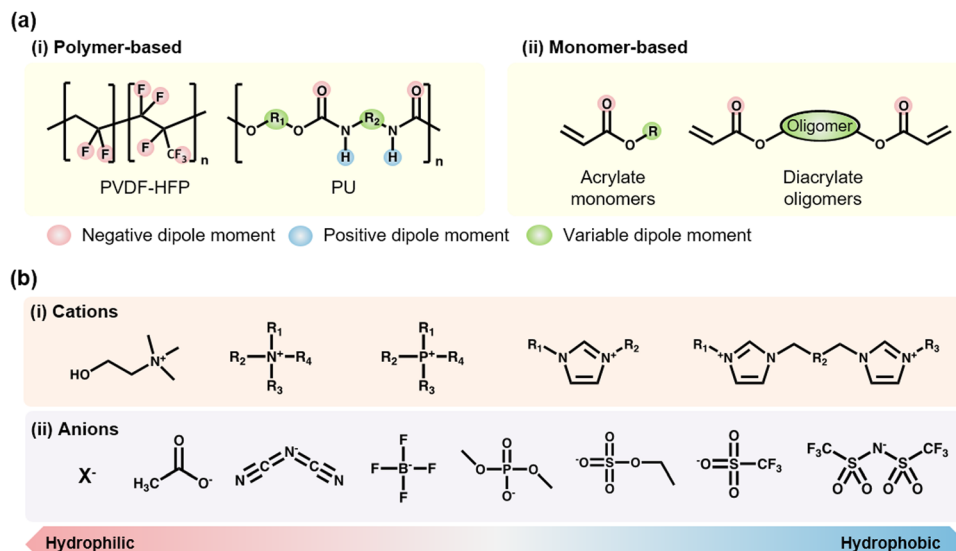


Fig. 7 Materials of Ionic liquid (IL)-based SICs (IL-SICs). (a) Representative polymers for IL-SICs (i) commercially available polymers, or (ii) monomers and oligomers, respectively. The coloured elements represent their relative dipole moment to show the possibility of interactions. (b) Representative cations and anions of ILs listed by their hydrophilicity.

(~45 mol%). The amorphous and polar  $-\text{CF}_3$  groups in HFP strongly interacted with the  $[\text{EMIM}^+]$  cation, and the ion-dipole interaction enabled soft, highly stretchable, and self-healable SICs (Fig. 8a). In a further study, by exchanging the anions with hydrophobic  $[\text{TFSI}^-]$ , Wang and Tee *et al.* developed SICs that enable underwater self-healable iontronics.<sup>74</sup>

Kim *et al.* reported a series of thermoplastic polyurethane (TPU)-based IL-SICs.<sup>81</sup> They mixed the TPU with the IL of  $[\text{EMIM}^+][\text{TFSI}^-]$ , where the mixtures were stabilized through the H-bonding between urethane groups and the  $[\text{EMIM}^+]$  cations. When the pressure was applied, the ILs squeezed out from the polyurethane networks and moved to the electrode by the visco-poroelastic mechanism, and the resulting ionic flow detected a pressure change (Fig. 8c). In a further study, they incorporated silanol-modified silica microparticles into the TPU-IL mixtures, where the H-bonding between the silica surfaces and the  $[\text{TFSI}^-]$  anions enhanced the ionic flow under mechanical stimuli.<sup>88</sup> As a result, they fabricated ultra-sensitive ionic mechanoreceptors, and they also demonstrated a wearable aerial drone microcontroller (Fig. 8d).

Unlike the as-synthesized polymer-based fabrications, when the IL-SICs are fabricated from monomer precursors, various-fabricating methods and diverse monomer combinations can be utilized. There exist many types of monomers (*e.g.*, vinyl monomers, acrylates, norbornenes, *etc.*), and the acrylate monomers are easy to polymerize *via* heat, and UV light, or click reactions. Therefore, researchers have designed various combinations of acrylate monomers with the ILs.<sup>89–109</sup>

Yan *et al.* reported IL-based click-ionogels.<sup>101</sup> They fabricated double network ionogels *via* thiol-ene Michael addition reactions. The ionogels were constructed by ionically cross-linked poly(1-butyl-3-vinyl imidazolium fluoroborate) and chemically cross-linked polyethylene glycol diacrylate (PEGDA) networks. The designed ionogels were mechanically tough

and highly stretchable, even at an extremely low temperature of  $-50^\circ\text{C}$  (Fig. 9a). Due to the wide temperature range of the liquid state of  $[\text{BMIM}^+][\text{BF}_4^-]$ , the ionogels exhibited thermal stability from  $-50$  to  $120^\circ\text{C}$ . Jiang *et al.* also reported ethyl acrylate (EA)-based double network ionogels (Fig. 9b). The polymer networks were stabilized by the H-bonding between the  $-\text{CH}_x$  group and  $[\text{TFSI}^-]$  anions.<sup>92</sup> The existence of H-bonding was evidenced by the shift in the FT-IR peak. The double network structures enabled tough mechanical properties. Chen *et al.* reported hydrophobic IL-SICs composed of fully hydrophobic materials,<sup>99</sup> which are polymers of *tert*-butyl acrylate, ILs of  $[\text{BMIM}^+][\text{TFSI}^-]$ , and silica nanoparticles (Fig. 9c). Yue *et al.* reported multi-functional ionogels composed of 2,2,2-trifluoroethyl acrylate (TFEA), AAm, and  $[\text{EMIM}^+][\text{TFSI}^-]$ .<sup>100</sup> They interacted through both H-bonding and ion-dipole interactions (Fig. 9d). Further, numerous studies have reported the virtue of synthetic variation of monomer-based IL-SICs.<sup>89,90,93–99,102–109</sup>

Recently, Sun *et al.* reported a triboresistive touch sensor based on the ionic PDMS.<sup>91</sup> The ionic PDMS in that study was composed of hydrophilic PDMS and hydrophobic IL through H-bonding and van der Waals interactions (Fig. 9e). In general, PDMS is a hydrophobic and nonpolar polymer, whereas the ILs are hydrophilic and polar materials. By lengthening the alkyl chain of the imidazolium cation and grafting the hydroxyl group on PDMS, they could be mixed homogeneously, resulting in ionically conductive PDMS. They fabricated skin-mountable, mono-layered, and grid-free triboresistive touch sensors based on the ionic PDMS, and they demonstrated the operation of a robot arm controller, which moves a leaning egg to a target spot through touch.

### 3.5. Liquid-free SICs

With the development of various SICs, researchers believed that a problem is that any liquid could leak. As a result, researchers

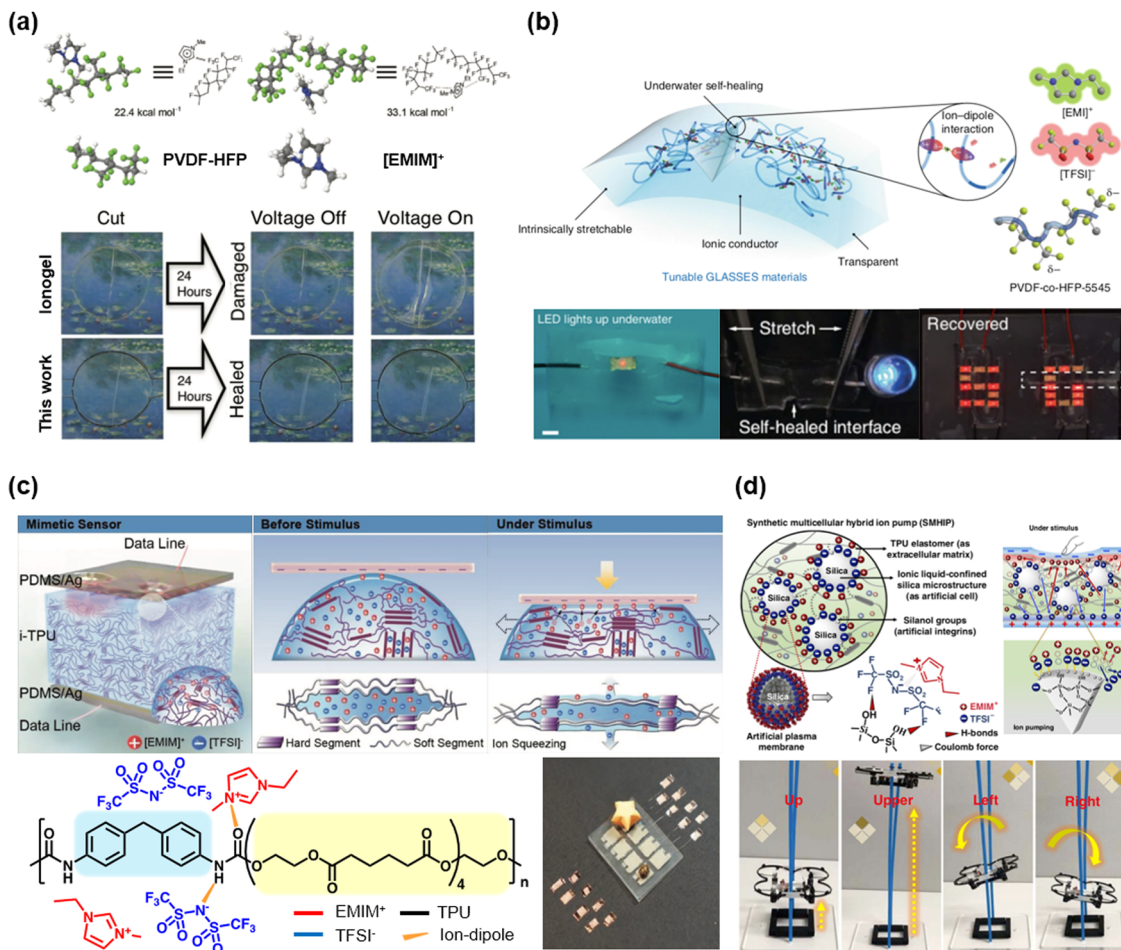


**Fig. 8** Representative synthesized polymer-based IL-SICs. (a and b) A poly(vinylidene fluoride-co-hexafluoropropylene) (PVDF-HFP) based IL-SICs for self-healable transparent SICs. PVDF-HFP could interact with  $[\text{EMIM}]^+$  through ion–dipole interaction, due to their strong  $-\text{CF}_3$  dipole unit. Reproduced with permission from ref. 52. Copyright 2016, Wiley-VCH. Reproduced with permission from ref. 74. Copyright 2019, Springer Nature. (c and d) Polyurethane (PU) based IL-SICs for iontronic sensor applications. The urethane group and  $[\text{EMIM}]^+[\text{TFSI}]^-$  could interact via ion–dipole interaction and hydrogen bonding. Due to the strong interactions, these IL-SICs are stable and applicable to stretchable devices. Reproduced with permission from ref. 84. Copyright 2017, Wiley-VCH. Reproduced with permission from ref. 88. Copyright 2019, Springer Nature.

have investigated the design of SICs without liquids to mitigate leakage, evaporation, and solvent exchange.

First, lithium ionic ( $\text{Li}^+$ ) salt-based SICs have been investigated.<sup>32,110–114</sup> The ionic conduction of  $\text{Li}^+$  can be facilitated by hopping or chain segmental motion of the ethylene oxide chains.<sup>115</sup> Studies have attempted to design the polymers in two ways based on whether the ethylene oxide groups are incorporated into the side-chain or the main chain (Fig. 10a).

A simple mixture of polyethylene oxide with lithium salt (e.g.  $\text{Li}^+\text{TFSI}^-$ ) is ionically conductive but not stretchable.<sup>117</sup> Therefore, researchers have designed copolymers. Ding *et al.* reported ionic-conducting elastomers composed of copolymers of *n*-butyl acrylate (BA) and oligoethylene glycol methyl ether acrylates (OEGMEA), and  $\text{Li}^+\text{TFSI}^-$ .<sup>110</sup> The BA and OEGMEAs provide elastomeric properties and lower  $T_g$ , thus enabling ionically conductive without liquids (Fig. 10b). Jia *et al.* reported another liquid-free ionic elastomer composed of copolymers of isobornyl acrylate (IBA) and 2-methoxyethyl acrylate (MEA) and  $\text{Li}^+\text{TFSI}^-$ .<sup>55</sup> As the high  $T_g$  of IBA chains gives a shape

memory effect, the ionic elastomers were self-healable and 3D printable.

In another study, by introducing microphase-separated structures, Zhang *et al.* reported highly conductive ionic elastomers.<sup>116</sup> Their copolymers were composed of 2,2,3,4,4,4-hexafluorobutyl acrylate (HFBA) and OEGMEA, where the Li ions favour the hydrophilic OEGMEA phase, while the TFSI anions favour the hydrophobic fluorinated HFBA phase. The selectively enriched  $\text{Li}^+$  domain gave high ionic conductivity to the elastomers. The compositionally optimized ionic elastomers also exhibited ultra-stretchability of over 60, high toughness, and self-healability.

In addition to side-chain design, main-chain engineering for SICs has also been investigated. Coincidentally, researchers in the field of lithium-based batteries have also investigated the development of liquid-free SICs to meet the demand for solid-state electrolytes for safe and non-flammable energy storage systems. Many studies on main-chain engineering liquid-free SICs can be found in the field of energy applications.<sup>32,112</sup>

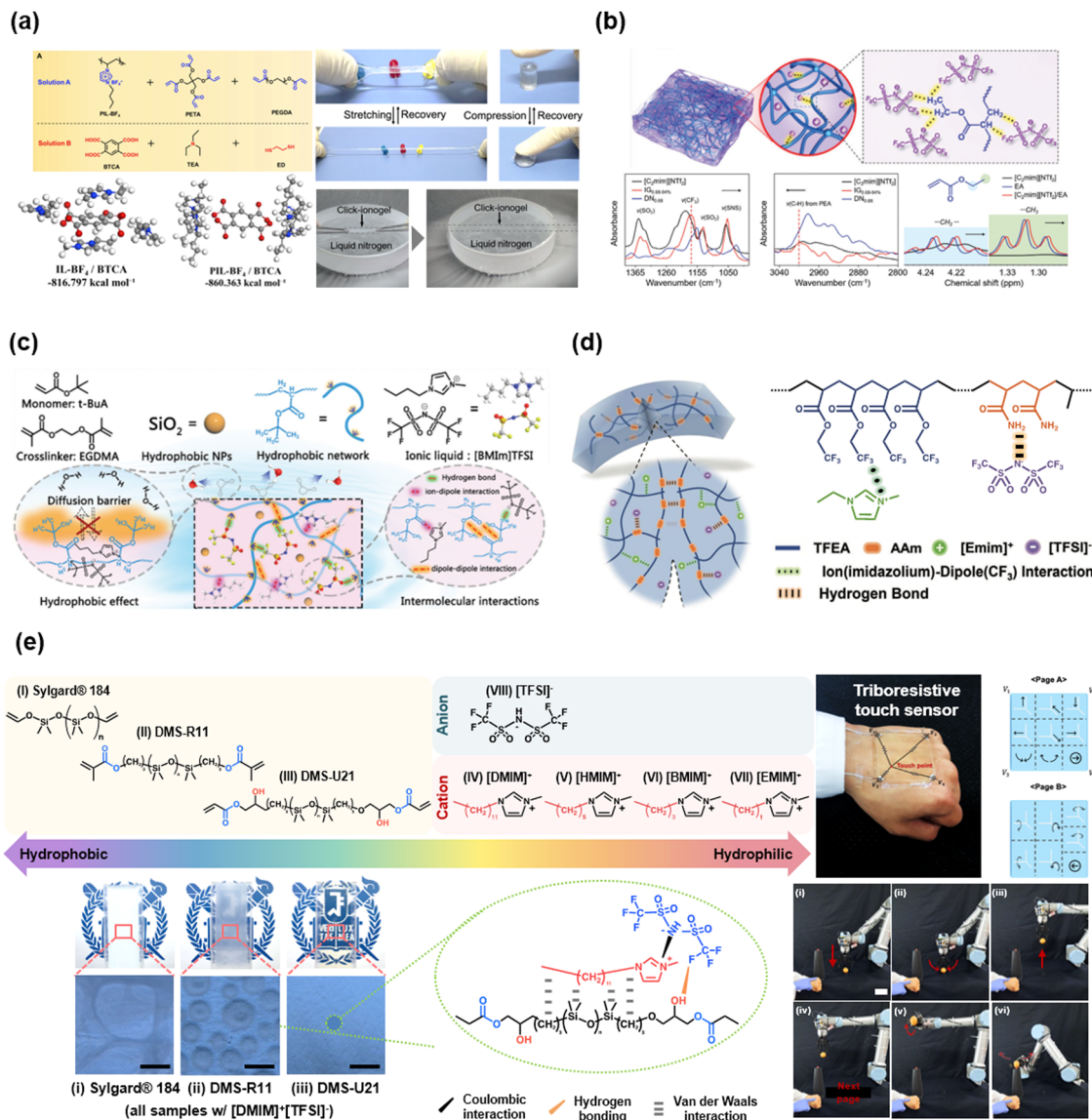


**Fig. 9** Representative acrylate or oligomer based IL-SICs. (a) Thiol-ene cross-linked double network click ionogels for stable iontronics. Reproduced with permission from ref. 101. Copyright 2019, AAAS. (b) Ethyl acrylate (EA) based double network ionogels, stabilized by hydrogen bonding between the alkyl group and ILs. Reproduced with permission from ref. 92. Copyright 2020, The Royal Society of Chemistry. (c) A fully hydrophobic IL-SICs for underwater communications. Reproduced with permission from ref. 99. Copyright 2021, The Royal Society of Chemistry. (d) Self-healable IL-SICs through hydrogen bonding and ion-dipole interaction Reproduced with permission from ref. 100. Copyright 2021, Wiley-VCH. (e) Ionic PDMS, which is based on hydrophilic PDMS and hydrophobic IL through hydrogen bonding and van der Waals interaction for triboresistive touch sensors. Reproduced with permission from ref. 91. Copyright 2022, Wiley-VCH.

Bao *et al.* reported supramolecular lithium-ion conductors composed of a soft segment of poly(propylene glycol)-poly(ethylene glycol)-poly(propylene glycol) (PPG-PEG-PPG) and strong quadruple hydrogen-bonding functional groups of 2-ureido-4-pyrimidone (UPy).<sup>32</sup> The UPy groups imparted mechanical strength to the conductors, while the Li<sup>+</sup> ions were conductive through the soft segments, therefore resulting in mechanically robust solid-state ionic conductors. They demonstrated fully stretchable batteries with supramolecular polymer networks (Fig. 10c).

Pu *et al.* reported a self-healable solid polymer electrolyte composed of end-group imine-functionalized PEG networks

and LiPF<sub>6</sub>.<sup>112</sup> The reversible imine bonds enabled a self-healing polymer electrolyte. They also demonstrated flexible pouch cells.

Various other liquid-free SICs have also been reported as well. For example, Zhu *et al.* reported poly(IL) (PIL)-based ionoelastomers, which were copolymerized with BA and [1-(6-acryloyloxyhexyl)-3-ethylimidazolium<sup>+</sup>][TFSI]<sup>-</sup>.<sup>110</sup> The ionoelastomers are transparent, stretchable, and ionically conductive. Interestingly, the DEA was more stably operated by the ionoelastomers than the general ionogels (Fig. 11a). The phenomenon is attributed to the liquid-free nature, as the IL would penetrate the dielectric layer under a high electric field.

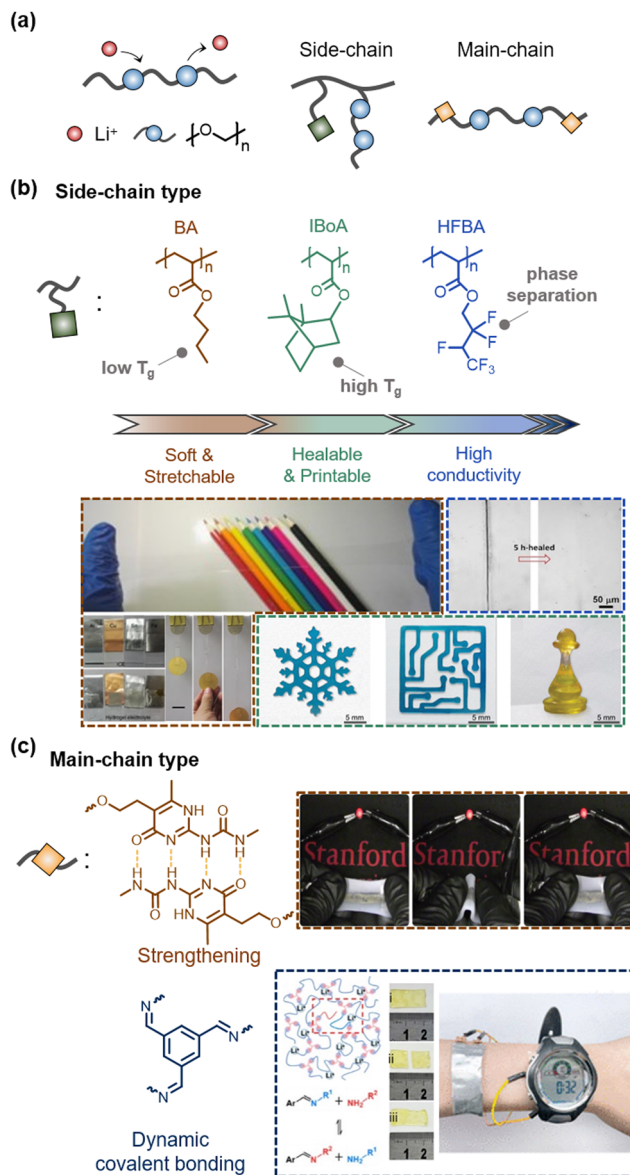


Fig. 10  $\text{Li}^+$ -Based liquid-free SICs. (a) Schematics of conduction mechanism and types of  $\text{Li}^+$ -based liquid-free SICs. (b) Examples of side-chain-type liquid-free SICs. Engineering co-monomers endows diverse properties to liquid-free SICs. Reproduced with permission from ref. 55. Copyright 2018, Springer Nature. Reproduced with permission from ref. 111 and 116. Copyright 2021, Wiley-VCH. (c) Examples of main-chain-type liquid-free SICs. Reproduced with permission from ref. 32. Copyright 2019, Springer Nature. Reproduced with permission from ref. 112. Copyright 2021, The American Chemical Society.

Researchers have also investigated polymerizable deep-eutectic-solvent (DES) systems for liquid-free SICs.<sup>118–125</sup> DESs are eutectic phases of certain binary mixtures, with negligible vapour pressure and thermal stability.<sup>120</sup> When the DESs consist of polymerizable monomers and ionic materials (not ILs), they are classified as polymerizable DESs, and they act as liquid-free SICs. A representative polymerizable ionic DES is a combination of acrylic acid (AAc) and choline chloride ( $\text{ChCl}$ ) (Fig. 11c). Wang *et al.* reported 3D printable solid-state

ionoelastomers composed of a polymerizable ionic DES, nanoclay, and light absorber.<sup>118</sup> The ionoelastomer networks interacted with the abundant H-bonding sites of the nanoclay, thereby constructing a robust ionic skeleton. They printed a 3D shape of piezoresistive sensors and stretchable microcircuits (Fig. 11d). Then, by adding AAm to the polymerizable ionic DESs, He *et al.* reported anti-freezing, self-healable, and mechanically robust ionoelastomers<sup>119</sup> (Fig. 11e).

In Sections 3.2–3.5, we have introduced various types of SICs by focusing on the types of their constituents. Each type has certain strengths and weaknesses, so we could properly choose the desired type of SICs for a required environment. From here, we introduce the other types of attractive SICs by focusing on the structures of polymer networks rather than their constituents.

### 3.6. Ampholytic materials of SICs

Ampholytes are materials that can be both acids and bases according to their circumstances. They are also classified as materials that have both positive and negative charges. Various types of ampholytes exist in nature: (i) zwitterion is a molecule that has both cation and anion, such as betaine or amino acids. (ii) Polyzwitterion is a polymer where the monomer contains both cation and anion, such as poly(sulfobetaines), poly(phosphocholines), or poly(imidazolium sulfonates). (iii) Polyampholyte is a polymer wherein the cationic monomers and the anionic monomers are copolymerized in a single network. (iv) Polyionic complex is a multiple polymer network where the polycations and the polyanions coexist (Fig. 12a). Researchers have utilized the interactions of ampholytic materials to design the SICs.

Wu *et al.* reported ionic hydrogel elastomers consisting of poly(acrylic acid) (PAA) and zwitterions.<sup>126</sup> The weakly complexed zwitterionic supramolecular network softens the initial stretch, showing skin-like strain-stiffening behaviours (Fig. 12b). The hydrogel elastomers exhibit high stretchability, negligible hysteresis, self-healability, re-processability, and adhesive properties, thus enabling the demonstration of iontronic sensors.

They also reported ultra-stretchable ionic conductors consisting of PAA, polyzwitterion of poly(3-dimethyl(methacryloyloxyethyl)ammonium propane sulfonate (PDMAPS), and IL of  $[\text{EMIM}]^+$ .<sup>127</sup> The ion-dipole interaction between the polyzwitterion and the IL stabilizes mixing, which is further optimized by the incorporation of PAA. The optimized ionic conductor showed ultra-stretchability ( $>100$ ), transparency, 3D-printability, and self-healability (Fig. 12c).

Sun *et al.* reported salt-mediated polyampholyte hydrogel ionic conductors.<sup>128</sup> They designed a cationic monomer to contain the imidazolium cation and the urea group, and copolymerizing it with the anionic SPA monomer in salty water. The polyampholyte hydrogels were formed by electrostatic interactions between cations and anions and hydrogen bonding between urea groups in cations. The hydrogels exhibited robust mechanical properties, self-healability, and ionic conductivities. As the complexation of cations and anions in polyampholytes increased *via* dialysis,<sup>53</sup> the hydrogels were also mechanically

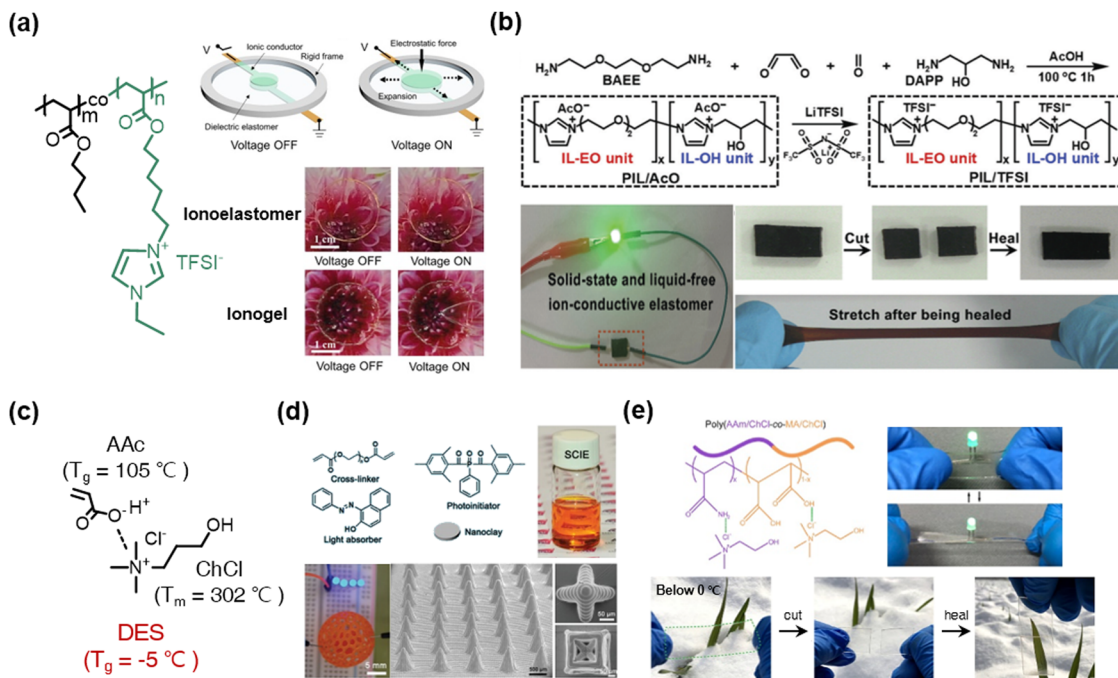


**Fig. 11** Poly(ionic liquid) (PIL)-based liquid-free SICs. (a) Acrylate-based PILs for stable operation of dielectric elastomer actuators. Reproduced with permission from ref. 110. Copyright 2021, The American Chemical Society. (b) Synthesis of main-chain-type imidazolium-based PILs. Reproduced with permission from ref. 114. Copyright 2020, The Royal Society of Chemistry. (c) A polymerizable ionic deep-eutectic solvent (DES) based on acrylic acid and choline chloride. (d) A 3D-printable DES-based PIL. Reproduced with permission from ref. 118. Copyright 2021, Wiley-VCH. (e) A DES-based anti-freezing PIL. Reproduced with permission from ref. 119. Copyright 2020, The American Chemical Society.

strengthened by the dialysis, while remaining self-healable and satisfactorily conductive (Fig. 12d).

Researchers have also reported a polyionic complex system based on PAA and poly(quaternized-dimethylaminoethyl acrylate) (PDMAEA-Q) (Fig. 12e). The polyionic complexes were stretchable, and printable, thus demonstrating artificial prosthetic skins.<sup>119</sup>

Ampholytic materials have been utilized to construct functional ionic materials.<sup>32,33,53,126–132</sup> Designing ampholytic materials combined with unique properties could lead to the development of superb iontronic materials.

### 3.7. Aligned iontronics based on liquid crystal elastomer (LCE)

A homogenously mixed system is typically amorphous. There have been various studies aiming to give iontronic materials a directionality or an anisotropy. They have accomplished this by adding ions into liquid crystalline elastomers (LCE), where liquid crystals (LCs) are incorporated in crosslinked polymer networks. The LCs, also called mesogens, exhibit stimuli-responsive behaviours by adjusting their orientations to external temperature, light, magnetic field, or mechanical stretch.<sup>133–135</sup> Therefore, researchers have investigated different ways to design aligned iontronics.

Madsen *et al.* reported liquid crystalline ionogels consisting of the LC network of poly(2,2'-disulfonyl-4,4'-benzidine terephthalamide) (PBDT) and the IL of  $[\text{EMIM}^+][\text{OTF}^-]$ .<sup>136</sup> As the PBDT can be aligned in the magnetic field, researchers

fabricated the aligned LCE ionogels by first aligning the PBDT aqueous solution and then exchanging the solvent with the IL (Fig. 13a). The LCE ionogels obtained in this way exhibited anisotropic structures (Fig. 13b and c) and corresponding anisotropic ionic conductivities (Fig. 13d).

Wu *et al.* reported a robust iontronic fibre (IonoLCE) consisting of a rigid mesogen of RM257, a soft chain spacer of 2,2'-ethylenedioxy diethanethiol (EDDET), a crosslinker of pentaerythritol tetrakis (3-mercaptopropionate) (PETMP), and an ionic liquid of  $[\text{BMIM}^+][\text{PF}_6^-]$ .<sup>137</sup> The diacrylate mesogens were reacted with the dithiol chain spacer and the tetraethiol crosslinkers *via* click Michael-addition reactions, in the presence of the IL (Fig. 13e). As the LC networks were stretched and aligned, the networks created partial smectic domains and formed ionic nanochannels, which enabled strain-induced ionic conductivity boost (Fig. 13f). They investigated the IonoLCE through molecular dynamics simulations, which confirmed that the cations are stabilized by the chain spacer, and the anions are stabilized by the mesogen networks (Fig. 13g). They demonstrated shape-discriminable strain sensing and photo-thermal actuation.

Numerous types of LCEs and ionic materials exist. Since the LCEs respond to different stimuli, such as light, heat, magnetic or electric fields, a combination of LC networks with ionic materials would enable diverse stimuli-responsive iontronics.

### 3.8. Phase separation strategies for SICs

When the two materials coexist but exhibit substantially different dissociation energies, in other words, when the  $\chi$  value of

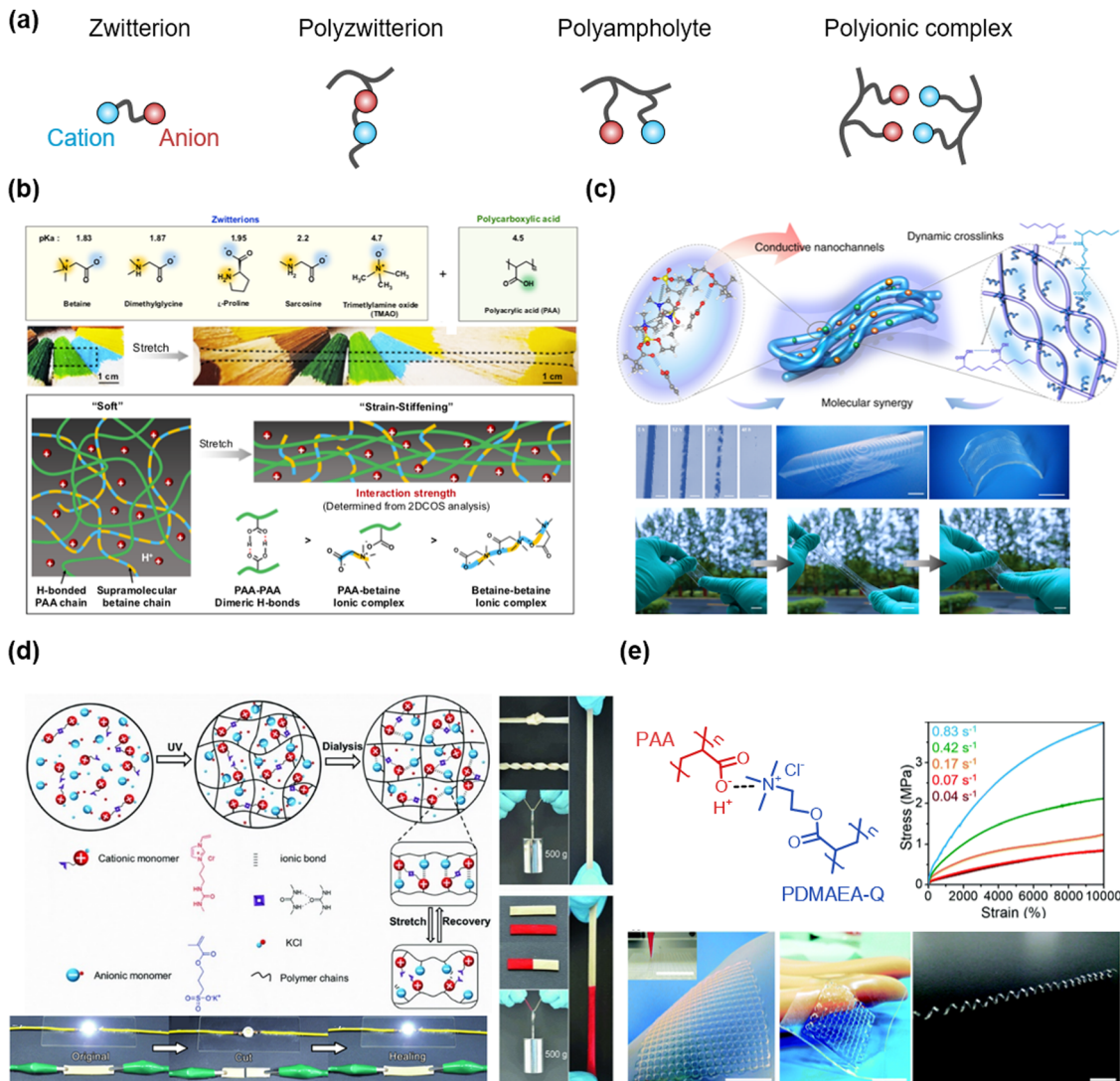


Fig. 12 Ampholytic materials for SICs. (a) Types of ampholytic materials. (b) Zwitterionic molecule-based SICs. Reproduced with permission from ref. 126. Copyright 2019, Springer Nature. (c) Polyzwitterion-based SICs. Reproduced with permission from ref. 127. Copyright 2021, Springer Nature. (d) Polyampholyte-based SICs. Reproduced with permission from ref. 128. Copyright 2018, Wiley-VCH. (e) Polyionic complex-based SICs. Reproduced with permission from ref. 129. Copyright 2019, The Royal Society of Chemistry.

the mixtures is high, the phase is separated. Each phase has distinct properties. Therefore, by adopting phase-separated morphologies, ionic materials having outstanding properties have been developed.<sup>138,139</sup>

Dickey *et al.* reported strong and tough ionogels through *in situ* phase separation.<sup>56</sup> The IL of  $[\text{EMIM}]^+$  is miscible with PAA networks, and immiscible with PAAm networks. (Fig. 14a) The optimized composition of the copolymer networks has two bicontinuous phases: (i) the polymer-rich domain dissipates mechanical energy and toughens *via* hydrogen bonding, and (ii) the solvent-rich domain provides stretchability to the ionogels (Fig. 14b and c). By mixing all monomers and polymerizing them with ultraviolet light, the researchers fabricated highly tough and stretchable *in situ* phase-separated ionogels by one-pot method, and these ionogels demonstrated robust mechanical properties, self-healability, and shape-memory properties.

Lee *et al.* reported elastomeric electrolytes for high-energy solid-state lithium batteries.<sup>140</sup> Solid-state electrolytes are important for the safe operation of lithium metal batteries, but they suffer from poor ionic conductivity and mechanical properties. The researchers designed elastomer electrolytes consisting of butyl acrylate (BA)-based elastomers and eutectic complexes of plastic crystals of succinonitrile (SN) and  $\text{Li}^+\text{TFSI}^-$  (Fig. 14d). By mixing all the monomers and having them *in situ* thermally polymerized within the battery structure, the electrolytes exhibit high conductivity, stretchability, and high adhesion energy *via* polymerization-induced phase separations. (Fig. 14e) The mechanical elasticity prevents the formation of dendrites (Fig. 14f), and the interconnected ionic phase enables high cumulative capacity and Coulombic efficiency, thus leading to lithium metal batteries with high specific energy.

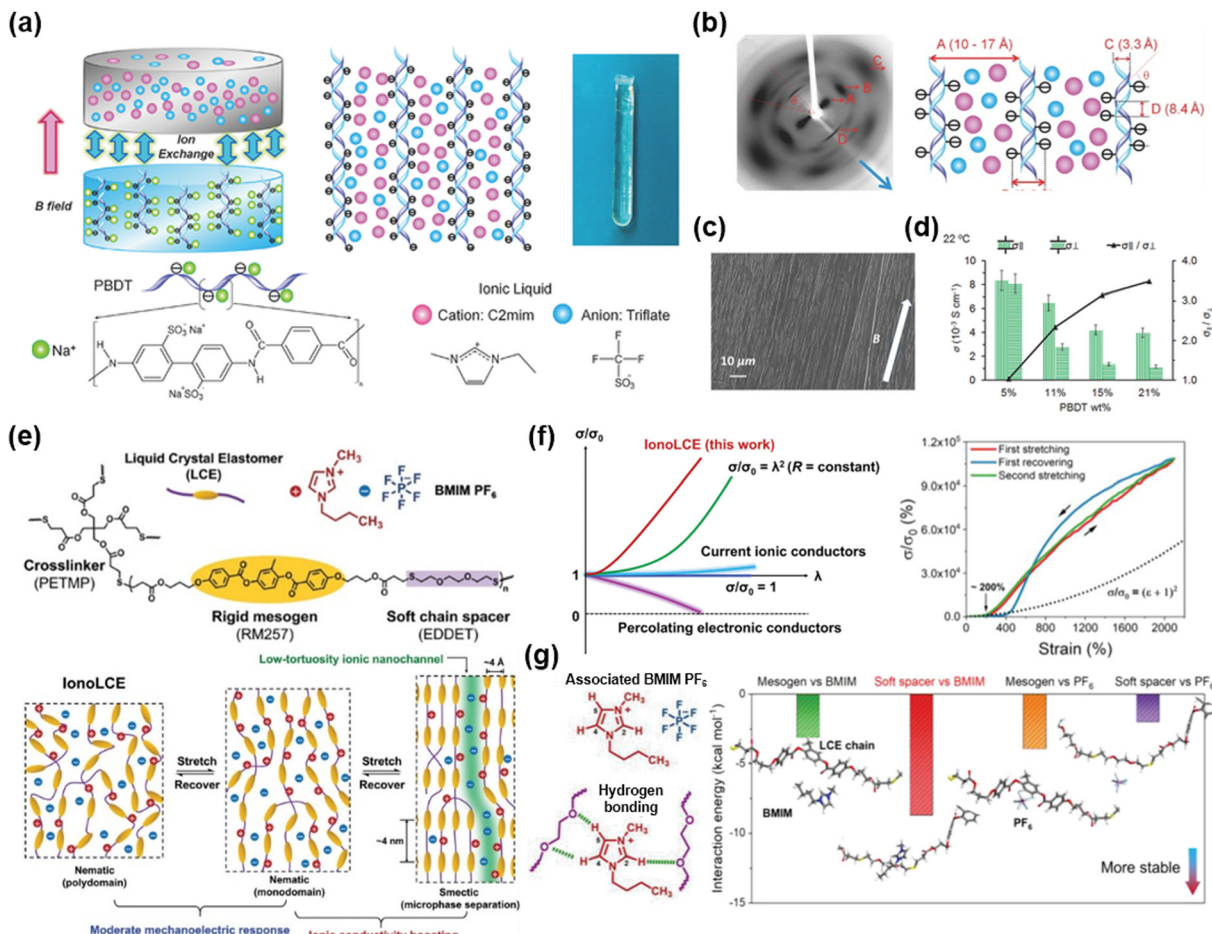


Fig. 13 Aligned iontronics based on liquid crystal elastomer (LCE)-IL composites. (a) A magnetically aligned PBDT-IL gel. (b) X-ray diffraction image of the gel and its correspondent diagram. (c) SEM image of the side-on surface of the gel. (d) Anisotropic ionic conductivity of the gel. Reproduced with permission from ref. 136. Copyright 2016, Wiley-VCH. (e) Molecular structures of the IonoLCE and schematics of stretch-induced ionic conductivity boost of the IonoLCE. (f) Mechanoelectric response of the IonoLCE and other ionic conductors. (g) Molecular interactions in the IonoLCE and calculated interaction energies. Reproduced with permission from ref. 137. Copyright 2021, Wiley-VCH.

Phase separation with bicontinuous structures would be able to give a material two distinct properties simultaneously. The design of stretchable iontronic materials with this strategy would open up new possibilities and opportunities for the development of superior ionic materials.

#### 4. Stretchable ionic semiconductors (SISs)

Conventional electronic semiconductors are doped by impurities. The doping enables electron-rich or hole-rich (or electron-poor) states in the electronic semiconductors, where the junction between them has electrical selectivity, and they operate as diodes and transistors. The diode and transistor show electrical switching behaviour, which is called rectification, and they construct the essential elements of computational electronic devices.<sup>141</sup>

In the case of iontronics since the charge carrier is ions, ion selectivity is needed for current switching. The polyelectrolyte networks immobilize a certain charge on the polymer networks,

while the counterpart charge is not bound to the networks and is relatively mobile. Therefore, the junction of the opposite polyelectrolyte networks would behave as an ionic rectifier.<sup>142</sup>

However, as the polyelectrolyte networks generally have high  $T_g$  due to numerous ionic pairs and their strong interactions,<sup>53</sup> the dry polyelectrolytes have low stretchability and high stiffness. Furthermore, as hard polymer networks restrict the chain segmental motions<sup>143</sup> and the ionic pairs are not solvated without solvents, the ionic conductivity is typically low in dry polyelectrolyte networks. Therefore, to provide stretchability and ionic conductivity, plasticizers should be added to the polyelectrolyte networks to untangle the networks and solvate the ionic pairs. Plasticized by water, polyelectrolyte hydrogels have been utilized as the SISs. To this end, the low  $\chi$  values between polyelectrolyte networks and plasticizers are preferred for the SISs.

##### 4.1. Phenomenon in polyelectrolyte junctions

When the anions are immobilized in the networks and the cations are free to move, the networks are called polycation,

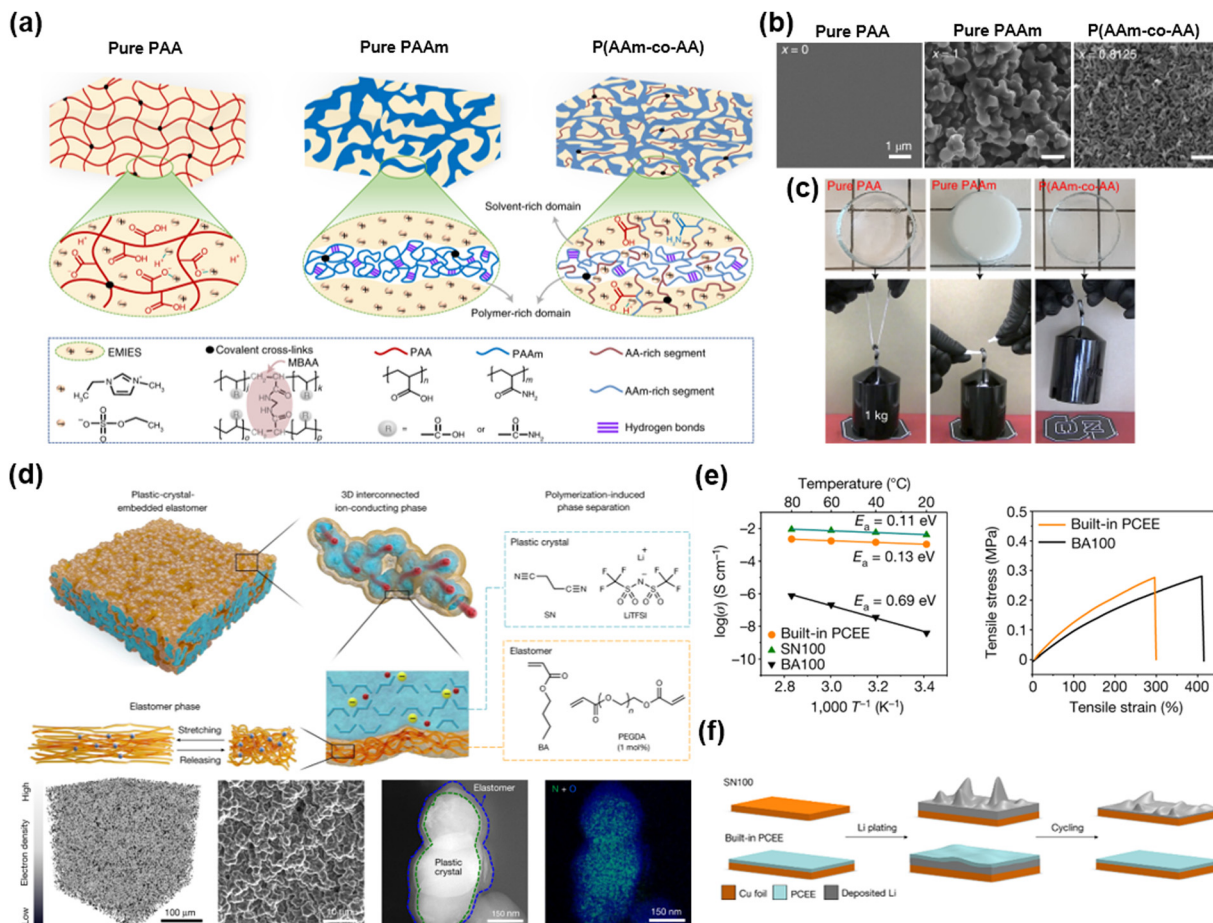


**Fig. 14** Phase separation strategies for superior ionic materials. (a) Schematics of three ionogels, where the first two are the homopolymer and the last is the phase-separated copolymer. (b) SEM images of the three ionogels. (c) Photographs of the three ionogels trying to lift a 1 kg weight. Reproduced with permission from ref. 56. Copyright 2022, Springer Nature. (d) Schematics and morphologies of the PCEE electrolytes. (e) The PCEE electrolytes have both high ionic conductivity and stretchability. (f) Schematics of Li plating and stripping with the different types of electrolytes. Reproduced with permission from ref. 140. Copyright 2022, Springer Nature.

and they are called polyanion in the opposite situation. When the polycation and the polyanion form a junction, it is called an ionic diode. At the junction of the electronic diode, the electrons and holes meet together and disappear. In the case of an ionic diode, on the other hand, the cations and anions do not disappear, rather they move across the junctions. If we place the ionic heterojunction between the reservoirs, connect it to electrodes, and apply bias voltages, (Fig. 15a) under the forward bias, the cations move to the negative electrode and the anions move to the positive electrode. In terms of the movement of cations, when the mobile cations enter into the polycationic region, they may be hindered by the fixed cations of the polycation. However, the mobile anions in the polycationic region neutralize charges, which generate current flow. The same way can be applied to the movement of anions. While under reverse bias, the movable ions in the polycation and polyanion move out to the reservoirs, and a depletion region is formed near the junction. At this point, due to the Donnan exclusion, the ions in the reservoir cannot be entered into the polyelectrolytes.<sup>144</sup>

Therefore, the ionic heterojunction shows rectifying behaviour under different biases.

#### 4.2. Materials development in stretchable ionic junctions

To realize the ionic junction with stretchable forms, researchers have utilized polyelectrolyte hydrogel junctions. The first hydrogel junction was reported by Velez *et al.* in 2007<sup>145</sup> (Fig. 15b). They physically mixed the polyanion of poly(styrenesulfonate) sodium salt (PSS) and the polycation of poly(diallyldimethylammonium) chloride (PDAC) with agarose hydrogels. The agarose helped retain the shape, and the mixed polyelectrolyte hydrogel junction showed nonlinear current responses.

Conventional polyelectrolyte hydrogels are mechanically poor due to their large-swelling ability due to high osmotic pressure and subsequently degraded mechanical properties.<sup>146</sup> Sun *et al.* reported co-polyelectrolyte hydrogels with chemically addressable polysaccharides.<sup>38</sup> By using methacrylated hyaluronic acid (HA) as co-polyanion with 3-sulfopropyl acrylate potassium salt (SPA), and methacrylated chitosan (CTS) as

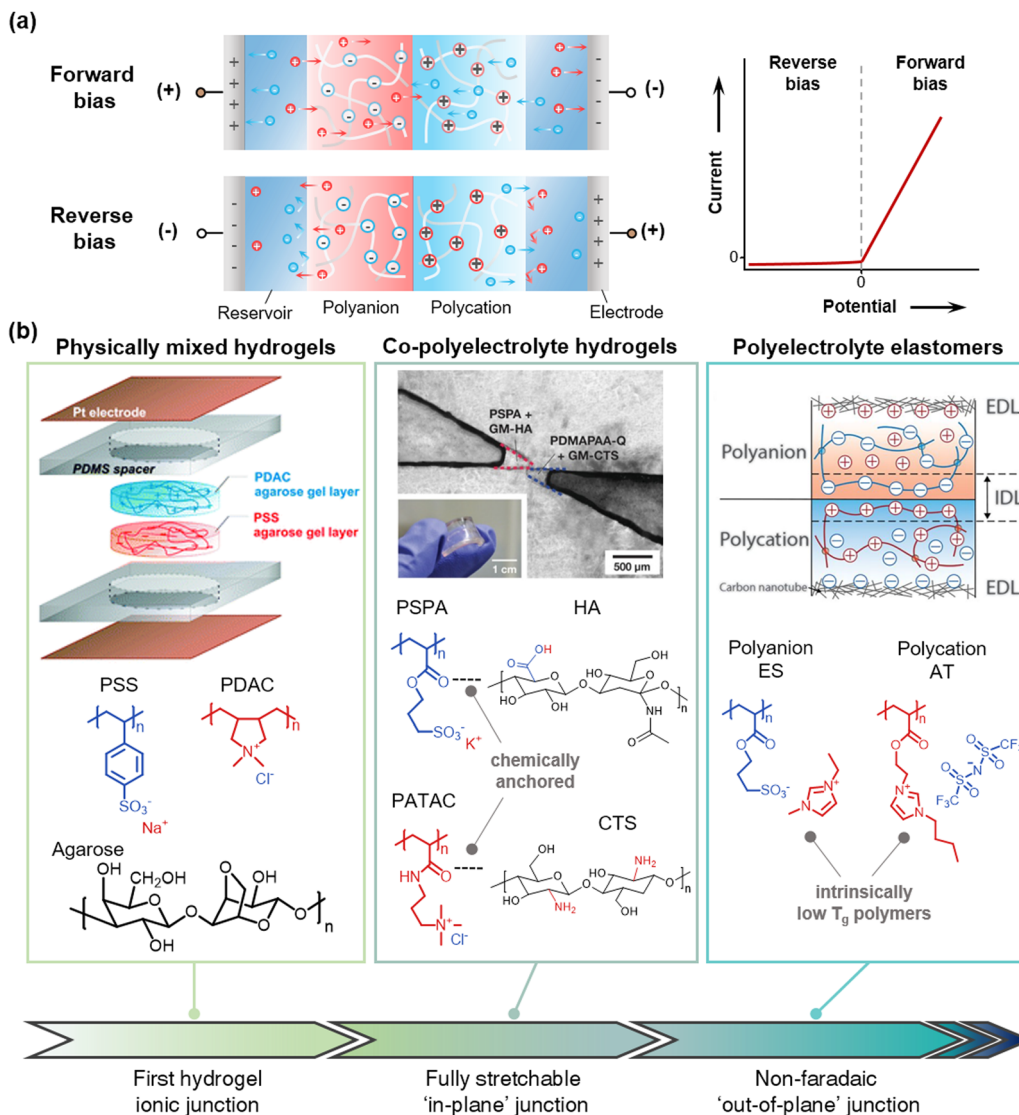


**Fig. 15** Materials development in stretchable polyelectrolyte junctions. (a) Schematics of polyelectrolyte ionic heterojunctions between polycations and polyanions. According to the bias direction, the ionic junction acts as an ionic semiconductor by rectifying current. (b) Development of the SISs. A first hydrogel ionic junction was achieved by mixing polyelectrolytes with agarose scaffold. Reproduced with permission from ref. 145. Copyright 2007, The American Chemical Society. Then, the in-plane junctions of co-polyelectrolyte hydrogels with chemical anchoring improve the mechanical and electrical performance. Reproduced with permission from ref. 38. Copyright 2018, Wiley-VCH. The out-of-plane junction of ionoelastomers enables non-faradaic rectification. Reproduced with permission from ref. 37. Copyright 2020, AAAS.

co-polycation with (3-acrylamidopropyl)trimethylammonium chloride (ATAC), the researchers enhanced the mechanical properties of polyelectrolyte hydrogels without the loss of ion selectivity. They demonstrated fully stretchable ionic diodes based on the hydrogels with VHB substrate (Fig. 15b).

Although there have been numerous efforts to fabricate ionic diodes or transistors,<sup>38,145,147–150</sup> they have suffered from the stability of liquid electrolytes, such as evaporation, leakage, or faradaic electrochemical processes. Suo *et al.* reported ionoelastomer junctions based on PILs.<sup>37</sup> They polymerized the cross-linked networks of 1-ethyl-3-methyl imidazolium-(3-sulfopropyl)acrylate (ES) as a polyanion and 1-[2-acryloyloxyethyl]-3-butylimidazolium bis(trifluoromethanesulfonyl)-imide (AT) as a polycation. As the polymers exhibit intrinsically

low  $T_g$  below 0 °C, they are intrinsically stretchable and ionically conductive without plasticizers at room temperature, and they have wide electrochemical windows based on the characteristics of ionic liquids. When further coupled with a high-surface-area carbon nanotube as an electrode/ionoelastomer interface, they demonstrated non-faradaic rectification *via* the out-of-plane junction, thus enabling stretchable diodes, transistors, and electro-mechanical transducers.

Furthermore, the junction of opposite polyelectrolytes generates an internal ionic flow under asymmetric charge concentrations. The power generation of polyelectrolyte junctions has also been studied with different ionic power sources<sup>30,151,152</sup> by ion concentration gradients,<sup>30,151</sup> and environmental humidity.<sup>152</sup>

The development of SISs has been harnessed from the paradigm by which biological systems use ions as charge carriers. Realizing synthetic ionic devices to enable 'real' communication with humans would be fascinating, yet there are still several hurdles that must be resolved, such as low ionic conductivity, low rectification ratio, or operational stabilities. Further studies are necessary to address these issues.

## 5. Stretchable ionic insulators (SIIIs)

Along with the development of ionically conductive materials, the role of ionic insulators has also been spotlighted. The SIIIs are placed between the SICs in the design of stretchable ionics. When the voltage is applied to each ionic conductor, the SIIIs should prevent the penetration of ions under an electric field, thus acting as a dielectric. The SII layer is crucial to operating stretchable iontronic devices because otherwise, an electrochemical reaction occurs under applied voltages. Because of this, the SIIIs have to keep ions from dissociating within them, in other words, the  $\chi$  value of SIIIs with ions should be high.

The capacitance  $C$  of the dielectric is proportional to the dielectric constant  $k$  of the dielectric, as  $C = k_0 k A/d$ , where  $k_0$  is the dielectric constant of vacuum,  $A$  is the area of the applied field, and  $d$  is the thickness of the dielectric. Therefore, under the same operating conditions, the higher- $k$  dielectrics take the electric field more effectively.

### 5.1. High- $k$ SIIIs for low-voltage optoelectronics

Zinc sulphide (ZnS) ionic crystals are semiconductors, where their band gap of 3.6 eV represents a photonic wavelength of 345 nm.<sup>153</sup> When the ZnS is doped with Cu<sup>+</sup>, Al<sup>3+</sup>, or Mn<sup>2+</sup>, they emit visible phosphorescent light with colours ranging from deep blue to orange depending on their doping ratio, and white colour from the combination of each colour. In particular, they emit light under an alternate-current (AC) electric field. Therefore, the doped ZnS has been used to fabricate AC electroluminescence (ACEL) devices.<sup>154</sup> As the device only needs two parallel electrodes and a phosphor layer between them, the ACEL device can be transformed into intrinsically stretchable devices with the SICs (Fig. 16a).

A first attempt to fabricate a stretchable ACEL device was conducted with stretchable electronics. Stretchable electrodes are silver nanowire dispersions on a polydimethylsiloxane (PDMS) substrate, and the stretchable phosphor layer is a physically mixed composite of PDMS and phosphor. However, the stretchability of the materials is limited to  $\sim 100\%$ .<sup>18</sup>

As the limit of stretchability is attributed to the stretchable electrodes, researchers have demonstrated highly stretchable (with stretchability over 4 to 16) ACEL devices with the SICs.<sup>26,155,156</sup> In those works, however, the luminance was low because the role of the dielectric layer was not considered. They used commercially available stretchable dielectrics, such as VHB,<sup>155</sup> PDMS,<sup>26</sup> or Ecoflex<sup>156</sup> with dielectric constants below 4.

As mentioned above, a high dielectric constant of the SII layers can effectively apply an electric field to the phosphors.

Therefore, researchers have developed diverse materials engineering for SIIIs to enhance their dielectric constant (Fig. 16b and c). In 2016, Tybrandt *et al.* reported a high- $k$  stretchable ACEL composite composed of PDMS with barium titanate (BaTiO<sub>3</sub> or BTO) nanoparticles, which exhibited ferroelectric behaviour and accordingly high dielectric constant (from  $\sim 100$  to over 10 000 according to their size and crystallinity).<sup>163</sup> The luminance of the high- $k$  composite was more than 7 times greater than that of the ACEL composite without BaTiO<sub>3</sub> under the same operating conditions.<sup>157</sup>

Nevertheless, the low dielectric constant of PDMS hinders the development of high- $k$  SIIIs. Kong *et al.* reported the effect of the dielectric constant of SII materials on the luminance of the devices.<sup>160</sup> To this end, they compared several commercial thermoplastic elastomers, such as hydrogenated styrene-ethylene-butylene-styrene (H-SEBS) triblock copolymers, thermoplastic polyurethane (TPU), or PVDF-HFP. The higher the dielectric constant, the brighter the luminance, as was theoretically expected. Park *et al.* reported an organic high- $k$  composite, composed of PU with high- $k$  surfactant Triton X-100 (Fig. 16d). The surfactant plasticizes the PU and facilitates self-recovery of mechanical damages, thus demonstrating self-healable and deformable ACEL devices.<sup>158</sup> Kong *et al.* developed the dispersity of BTO by attaching a hydrophilic PVP ligand on its surface to enhance the miscibility with PVDF-HFP elastomers.<sup>161</sup> The strategy greatly reduced the operational voltages and demonstrated an epidermal stretchable stopwatch display. B. Tee *et al.* reported self-healable fluorinated high- $k$  composites, composed of PVDF-HFP with fluorosurfactant Zonyl FS-300 (Fig. 16d). The composite exhibited a high dielectric constant, self-healing ability, and good adhesion with PVDF-HFP-based ionic conductors, thus demonstrating the self-healable and extremely stretchable low-voltage ACEL device, and its integration into soft robots.<sup>162</sup> Zhu *et al.* reported transparent high- $k$  composites composed of PDMS and an immiscible IL of [1-propyl-3-methylimidazolium (PrMIm<sup>+</sup>)][TFSI<sup>-</sup>]. If the PDMS and IL are miscible, they act as an electrolyte. As the IL is solely dispersed in the PDMS with no solvation, the composites act as a dielectric. Furthermore, since the ILs are conductive, the electric field is concentrated on adjacent domains. By adding 4-fluoro-1,3-dioxolan-2-one to adjust the refractive index of the internal phase, the researchers ultimately demonstrated transparent high- $k$  SIIIs and their application to bright ACEL devices.<sup>159</sup>

Although we only introduce ACEL devices to meet the need for the development of high- $k$  SIIIs, high- $k$  materials can also be important in the design of transistors<sup>164</sup> or electro-actuators.<sup>165</sup> Existing studies with high- $k$  SIIIs have mainly taken two approaches: (i) composites with inorganic additives,<sup>161,163</sup> (ii) organic composites with high- $k$  materials,<sup>158,162</sup> or (iii) dispersions of immiscible conductive materials into dielectrics<sup>159</sup> (Fig. 16c). Understandably, high- $k$  polymers have highly polarized groups that strongly interact with each other, thus making the polymers brittle. Furthermore, since the high- $k$  materials are polar, they easily dissociate ions, and as a result, electric failure could occur more easily under a high

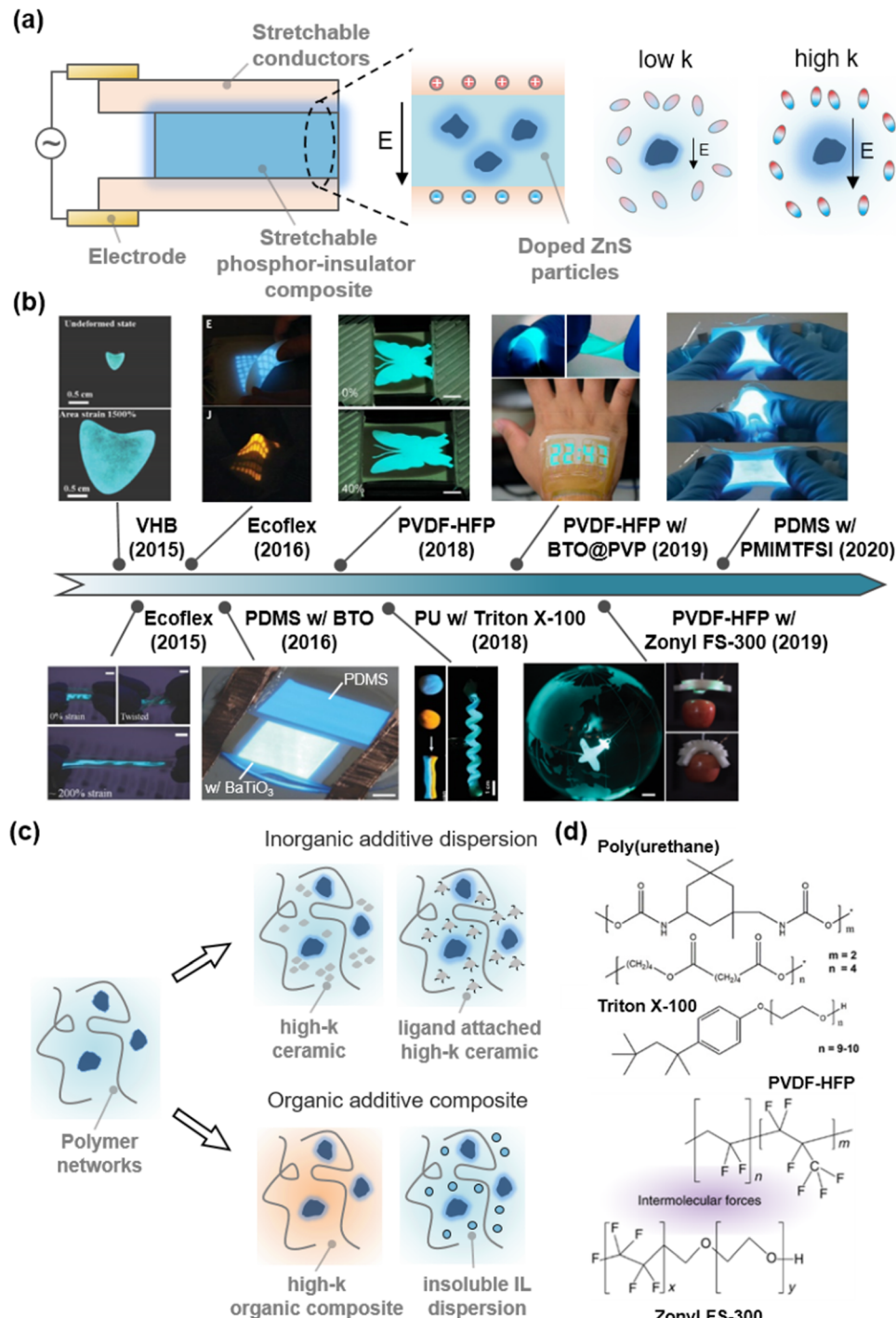


**Fig. 16** High- $k$  SIs for low-voltage optoelectronics. (a) Structure of stretchable alternate-current-electroluminescence (ACEL) devices. The phosphors exhibit higher luminescence under an electric field, when the surrounding medium has higher dielectric constants. (b) Materials development for low voltage stretchable ACEL devices. Reproduced with permission from ref. 155, 156, 157, 158 and 159. Copyright 2015, 2016, 2018, and 2020, Wiley-VCH. Reproduced with permission from ref. 26. Copyright 2016, AAAS. Reproduced with permission from ref. 160 and 161. Copyright 2018, and 2019, The American Chemical Society. (c) Schematics of strategies used to develop high- $k$  stretchable dielectrics. (d) Molecular structures comprising high- $k$  organic composites. Reproduced with permission from ref. 162. Copyright 2019, Springer Nature.

electric field. There is a trade-off between softness and polarity, and another trade-off between efficiency and stability for the device operation.

Therefore, it will be a challenge to design intrinsically soft high- $k$  'ionic' insulators. The development of such materials will open new opportunities in stretchable iontronics.

## 5.2. Low-*k* SIIIs for stable perovskite ionic crystals

In addition to the development of high-*k* SIIIs, low-*k* SIIIs have also been investigated. In terms of ionic crystals; their dissociation constant depends on the dielectric constant of the medium. In a high-*k* medium, the ionic crystals are dissociative, whereas, in a low-*k* medium, the ionic crystals are associative (Fig. 17a). The relationship between the dielectric constant of the

medium and the dissociation constant of the ionic crystals is represented in Fig. 17b.<sup>166</sup> For example, when *k* is 3.16, which is the value for poly(methyl methacrylate), the dissociation constant *D* is  $\sim 10^{-12}$ , while, when *k* is 46.7, which is the value that is almost that of the polar solvent DMSO, *D* is around zero. Some ionic crystals behave as a semiconductor, in which case their crystallinity greatly affects their properties. Therefore, for

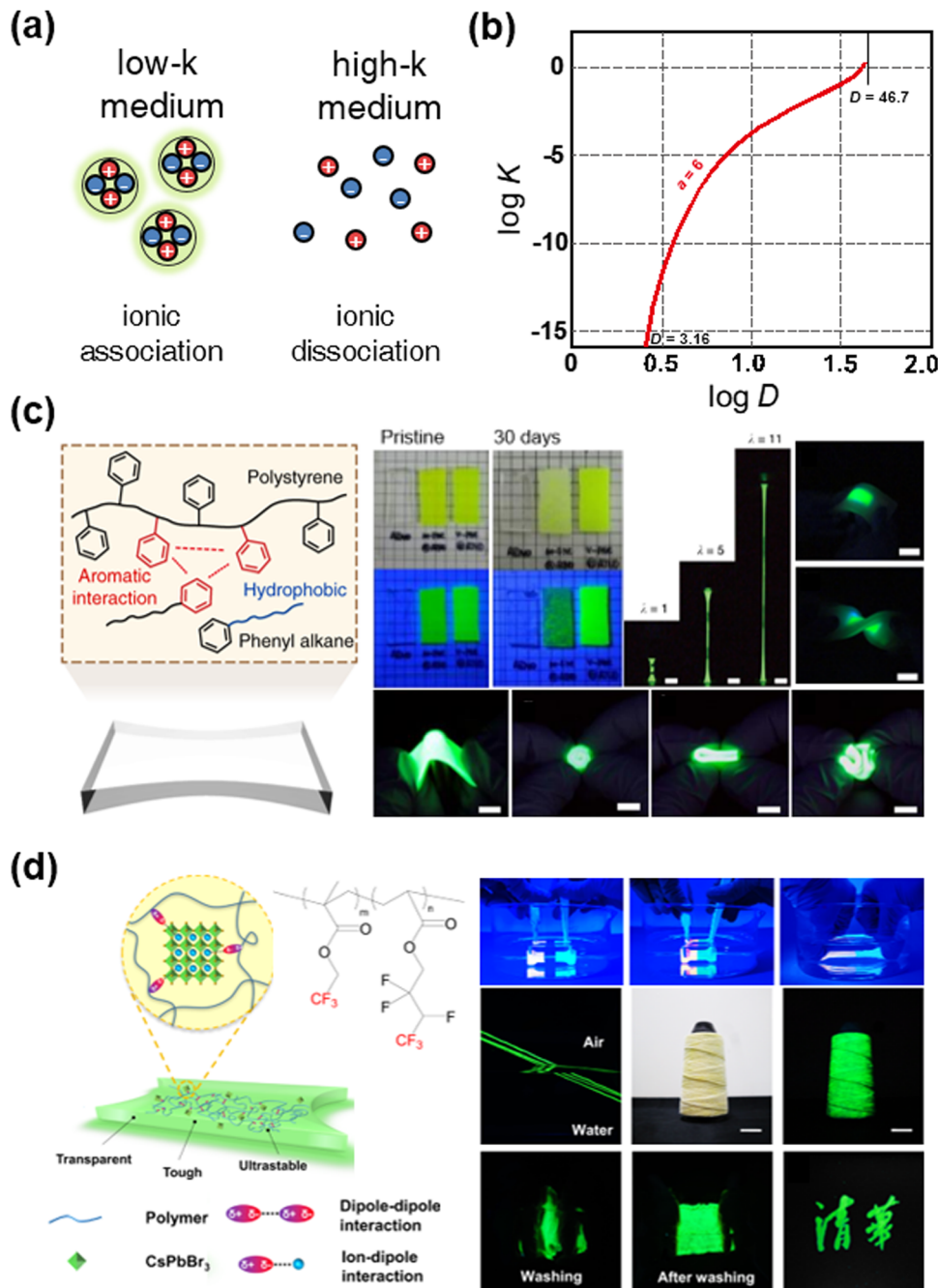


**Fig. 17** Low-*k* SIIIs for stable perovskite ionic crystals. (a) Schematics of the state of ionic crystals in different dielectric media. (b) The relationship between the ionic dissociation constant *D* and *k*. Reproduced with permission from ref. 166. Copyright 1955, The American Chemical Society. (c) Aromatic interaction-induced nonpolar organogels for efficient and stable perovskite emitters. Reproduced with permission from ref. 167. Copyright 2020, Springer Nature. (d) Dipole interaction-induced perovskite nanocomposites for stable and self-healable perovskite emitters. Reproduced with permission from ref. 168. Copyright 2022, Nature.

the stability and properties of ionic crystals, low- $k$  SIIIs will be needed.

Perovskite nanocrystals (PNCs) have recently attracted substantial attention, due to their high optical efficiency, narrow bandwidth, low material cost, and facile synthetic procedure.<sup>169</sup> However, their formation energy is low, which makes the PNCs highly unstable under ambient conditions. To resolve this issue, researchers have encapsulated PNCs with commercial low- $k$  materials.<sup>170–173</sup> However, these materials are often mechanically rigid,<sup>170,171</sup> or some stretchable materials did not efficiently encapsulate PNCs.<sup>172,173</sup>

Sun *et al.* reported aromatic interaction-induced nonpolar organogels for efficient and stable perovskite emitters (Fig. 17c). In general, the formation of low- $k$  gels is limited due to the weak intermolecular forces of low- $k$  materials, which leads to weak mechanical properties or solvent leakage. By introducing aromatic interactions to the polymer–solvent mixture system, researchers have fabricated highly stretchable, soft, transparent, and nonpolar organogels.<sup>167</sup> By encapsulating the PNCs covalently to the organogel networks, nanocomposites showed high photoluminescence efficiency (above 92% to 100%), stability under various environmental conditions (more than 100 days in the air, water, acid, and base), and softness and stretchability (Young's modulus  $\sim$  100 kPa and stretchability  $\sim$  11). They demonstrated intrinsically soft pure green electroluminescent devices.

Wang *et al.* reported tough and self-healable dipole–dipole interaction-induced elastomers (Fig. 17d). As the  $-\text{CF}_3$  functional groups have highly negative dipole moments, they can interact with each other, and the PNCs of the positively charged surface. The fabricated nanocomposites were mechanically tough and self-healable, and they showed stable luminescence. The researchers demonstrated stable pure green luminescent films and textiles.

It is important to develop low- $k$  soft materials for device passivation. For the development of stretchable integrated devices, especially displays where the constituents are highly unstable under ambient conditions, the development of SIIIs would provide environmental stabilities under operation.<sup>168</sup>

## 6. Conclusion and outlook

Stretchable iontronics offers new opportunities for ultimate human-oriented devices. For the material design of each component, researchers have considered mixing materials. They find proper solvents, ionic sources, polymer precursors, or other functional additives and then properly combine them to form homogeneous ionic functional materials. In some cases, they used immiscible combinations for phase-separated morphologies. In these processes, the library of molecular interactions was utilized to investigate and explain the mixing behaviours.

Hurdles would be the trade-off of the required properties in each ionic component. For the SICs and SIIIs, the ionic conductivity trades off with environmental stabilities. The presence

of liquids promotes ion solvation and enhances diffusivity and conductivity, while the liquids themselves are volatile or flammable. For the SIIIs, the high- $k$  environment increases the capacitive efficiency, whereas the ions are not associative in the high- $k$  nature. The realization of liquid-free highly ionic conductive materials, or high- $k$  ion-repulsive insulators, would be achieved by having a comprehensive understanding of the intermolecular interactions between diverse types of ions and polymers.

One challenge will be the discovery of newly applicable molecular interactions and functional groups. While there have been numerous studies, most of them have simply combined or slightly modified the previously reported materials. Although it is important to understand the interactions in newly mixed systems, the materialization of new functional groups greatly expands the branches of interactions in multi-component systems. To initiate new material design, as an example, it could be an opportunity to consider the molecular interactions in biological systems, since they are molecularly designed with complexity and sophistication.

This paper covered the development of materials to be used for stretchable iontronics, but the present insight and rules of materials design are not applicable only to iontronic materials. For the development of materials, molecular interaction is the most fundamental and must be understood, and it is just as challenging. Numerous elements exist in nature, and we should aim to exploit and utilize them to find currently unexplored functional groups and materials for the progress of stretchable iontronics, materials science, and humankind.

## Author contributions

J.-M. Park and S. Lim contributed equally to this work. J.-M. Park and S. Lim conceived this work, designed figures, and organized the outline of the manuscript. J.-Y. Sun supervised this work. All authors discussed this work and wrote the manuscript.

## Conflicts of interest

There are no conflicts to declare.

## Acknowledgements

This work was supported by LG Display under LGD-SNU Incubation Program. This work was supported by a National Research Foundation of Korea (NRF) grant funded by the Korean Government (2018M3A7B4089670 and 2021R1A2C2092737). The institute of Engineering Research at Seoul National University provided research facilities for this work.

## Notes and references

- 1 T. B. Singh and N. S. Sariciftci, *Annu. Rev. Mater. Res.*, 2006, 36, 199–230.

2 J. A. Rogers, T. Someya and Y. Huang, *Science*, 2010, **327**, 1603–1607.

3 M. L. Hammock, A. Chortos, B. C. K. Tee, J. B. H. Tok and Z. Bao, *Adv. Mater.*, 2013, **25**, 5997–6038.

4 D.-H. Kim, N. Lu, R. Ma, Y.-S. Kim, R.-H. Kim, S. Wang, J. Wu, S. M. Won, H. Tao and A. Islam, *Science*, 2011, **333**, 838–843.

5 D. J. Lipomi, M. Vosgueritchian, B. C. Tee, S. L. Hellstrom, J. A. Lee, C. H. Fox and Z. Bao, *Nat. Nanotechnol.*, 2011, **6**, 788–792.

6 H.-H. Chou, A. Nguyen, A. Chortos, J. W. To, C. Lu, J. Mei, T. Kurosawa, W.-G. Bae, J. B.-H. Tok and Z. Bao, *Nat. Commun.*, 2015, **6**, 1–10.

7 J. Kim, M. Lee, H. J. Shim, R. Ghaffari, H. R. Cho, D. Son, Y. H. Jung, M. Soh, C. Choi and S. Jung, *Nat. Commun.*, 2014, **5**, 1–11.

8 R. H. Baughman, C. Cui, A. A. Zakhidov, Z. Iqbal, J. N. Barisci, G. M. Spinks, G. G. Wallace, A. Mazzoldi, D. De Rossi and A. G. Rinzler, *Science*, 1999, **284**, 1340–1344.

9 S. Rosset and H. R. Shea, *Appl. Phys. A*, 2013, **110**, 281–307.

10 J. Xu, S. Wang, G.-J. N. Wang, C. Zhu, S. Luo, L. Jin, X. Gu, S. Chen, V. R. Feig and J. W. To, *Science*, 2017, **355**, 59–64.

11 N. Liu, A. Chortos, T. Lei, L. Jin, T. R. Kim, W.-G. Bae, C. Zhu, S. Wang, R. Pfattner and X. Chen, *Sci. Adv.*, 2017, **3**, e1700159.

12 S. Wang, J. Xu, W. Wang, G.-J. N. Wang, R. Rastak, F. Molina-Lopez, J. W. Chung, S. Niu, V. R. Feig and J. Lopez, *Nature*, 2018, **555**, 83–88.

13 Y. Dai, H. Hu, M. Wang, J. Xu and S. Wang, *Nat. Electron.*, 2021, **4**, 17–29.

14 H. L. Filiatrault, G. C. Porteous, R. S. Carmichael, G. J. Davidson and T. B. Carmichael, *Adv. Mater.*, 2012, **24**, 2673–2678.

15 T. Sekitani, H. Nakajima, H. Maeda, T. Fukushima, T. Aida, K. Hata and T. Someya, *Nat. Mater.*, 2009, **8**, 494–499.

16 M. S. White, M. Kaltenbrunner, E. D. Głowacki, K. Gutnichenko, G. Kettler, I. Graz, S. Aazou, C. Ulbricht, D. A. Egbe and M. C. Miron, *Nat. Photonics*, 2013, **7**, 811–816.

17 J. Liang, L. Li, X. Niu, Z. Yu and Q. Pei, *Nat. Photonics*, 2013, **7**, 817–824.

18 J. Wang, C. Yan, K. J. Chee and P. S. Lee, *Adv. Mater.*, 2015, **27**, 2876–2882.

19 J. Y. Oh, S. Rondeau-Gagné, Y.-C. Chiu, A. Chortos, F. Lissel, G.-J. N. Wang, B. C. Schroeder, T. Kurosawa, J. Lopez and T. Katsumata, *Nature*, 2016, **539**, 411–415.

20 Z. Zhang, W. Wang, Y. Jiang, Y.-X. Wang, Y. Wu, J.-C. Lai, S. Niu, C. Xu, C.-C. Shih and C. Wang, *Nature*, 2022, **603**, 624–630.

21 Y. Jiang, Z. Zhang, Y.-X. Wang, D. Li, C.-T. Coen, E. Hwaun, G. Chen, H.-C. Wu, D. Zhong and S. Niu, *Science*, 2022, **375**, 1411–1417.

22 C. Keplinger, J.-Y. Sun, C. C. Foo, P. Rothemund, G. M. Whitesides and Z. Suo, *Science*, 2013, **341**, 984–987.

23 J. Y. Sun, C. Keplinger, G. M. Whitesides and Z. Suo, *Adv. Mater.*, 2014, **26**, 7608–7614.

24 C.-C. Kim, H.-H. Lee, K. H. Oh and J.-Y. Sun, *Science*, 2016, **353**, 682–687.

25 I. You, D. G. Mackanic, N. Matsuhisa, J. Kang, J. Kwon, L. Beker, J. Mun, W. Suh, T. Y. Kim and J. B.-H. Tok, *Science*, 2020, **370**, 961–965.

26 C. Larson, B. Peele, S. Li, S. Robinson, M. Totaro, L. Beccai, B. Mazzolai and R. Shepherd, *Science*, 2016, **351**, 1071–1074.

27 X. Shi, X. Zhou, Y. Zhang, X. Xu, Z. Zhang, P. Liu, Y. Zuo and H. Peng, *J. Mater. Chem. C*, 2018, **6**, 12774–12780.

28 D. Y. Kim, S. Choi, H. Cho and J. Y. Sun, *Adv. Mater.*, 2019, **31**, 1804080.

29 H. S. Kang, S. W. Han, C. Park, S. W. Lee, H. Eoh, J. Baek, D.-G. Shin, T. H. Park, J. Huh and H. Lee, *Sci. Adv.*, 2020, **6**, eabb5769.

30 T. B. Schroeder, A. Guha, A. Lamoureux, G. VanRenterghem, D. Sept, M. Shteing, J. Yang and M. Mayer, *Nature*, 2017, **552**, 214–218.

31 Y. Lee, S. H. Cha, Y.-W. Kim, D. Choi and J.-Y. Sun, *Nat. Commun.*, 2018, **9**, 1–8.

32 D. G. Mackanic, X. Yan, Q. Zhang, N. Matsuhisa, Z. Yu, Y. Jiang, T. Manika, J. Lopez, H. Yan and K. Liu, *Nat. Commun.*, 2019, **10**, 1–11.

33 O. Kim, H. Kim, U. H. Choi and M. J. Park, *Nat. Commun.*, 2016, **7**, 1–8.

34 E. Acome, S. K. Mitchell, T. Morrissey, M. Emmett, C. Benjamin, M. King, M. Radakovitz and C. Keplinger, *Science*, 2018, **359**, 61–65.

35 Y. Lee, W. J. Song, Y. Jung, H. Yoo, M.-Y. Kim, H.-Y. Kim and J.-Y. Sun, *Sci. Robot.*, 2020, **5**, eaaz5405.

36 H. J. Kim, L. Paquin, C. W. Barney, S. So, B. Chen, Z. Suo, A. J. Crosby and R. C. Hayward, *Adv. Mater.*, 2020, **32**, 2000600.

37 H. J. Kim, B. Chen, Z. Suo and R. C. Hayward, *Science*, 2020, **367**, 773–776.

38 H. R. Lee, J. Woo, S. H. Han, S. M. Lim, S. Lim, Y. W. Kang, W. J. Song, J. M. Park, T. D. Chung and Y. C. Joo, *Adv. Funct. Mater.*, 2019, **29**, 1806909.

39 C. Yang and Z. Suo, *Nat. Rev. Mater.*, 2018, **3**, 125–142.

40 H. R. Lee, C. C. Kim and J. Y. Sun, *Adv. Mater.*, 2018, **30**, 1704403.

41 H. Wang, Z. Wang, J. Yang, C. Xu, Q. Zhang and Z. Peng, *Macromol. Rapid Commun.*, 2018, **39**, 1800246.

42 P. J. Flory, *Principles of polymer chemistry*, Cornell University Press, 1953.

43 C. M. Hansen, *Hansen solubility parameters: a user's handbook*, CRC Press, 2007.

44 A. A. Zavitsas, *J. Phys. Chem.*, 1987, **91**, 5573–5577.

45 A. J. Neel, M. J. Hilton, M. S. Sigman and F. D. Toste, *Nature*, 2017, **543**, 637–646.

46 R. Holyst, *Soft Matter*, 2005, **1**, 329–333.

47 J. C. Biffinger, H. W. Kim and S. G. DiMagno, *ChemBioChem*, 2004, **5**, 622–627.

48 V. H. Dalvi and P. J. Rossky, *Proc. Natl. Acad. Sci. U. S. A.*, 2010, **107**, 13603–13607.

49 Y. Cao, H. Wu, S. I. Allec, B. M. Wong, D. S. Nguyen and C. Wang, *Adv. Mater.*, 2018, **30**, 1804602.

50 T. Steiner, *Angew. Chem., Int. Ed.*, 2002, **41**, 48–76.

51 A. Chagnes, S. Nicolis, B. Carré, P. Willmann and D. Lemordant, *ChemPhysChem*, 2003, **4**, 559–566.

52 Y. Cao, T. G. Morrissey, E. Acome, S. I. Allec, B. M. Wong, C. Keplinger and C. Wang, *Adv. Mater.*, 2017, **29**, 1605099.

53 T. L. Sun, T. Kurokawa, S. Kuroda, A. B. Ihsan, T. Akasaki, K. Sato, M. Haque, T. Nakajima and J. P. Gong, *Nat. Mater.*, 2013, **12**, 932–937.

54 B. Chen, J. J. Lu, C. H. Yang, J. H. Yang, J. Zhou, Y. M. Chen and Z. Suo, *ACS Appl. Mater. Interfaces*, 2014, **6**, 7840–7845.

55 L. Shi, T. Zhu, G. Gao, X. Zhang, W. Wei, W. Liu and S. Ding, *Nat. Commun.*, 2018, **9**, 1–7.

56 M. Wang, P. Zhang, M. Shamsi, J. L. Thelen, W. Qian, V. K. Truong, J. Ma, J. Hu and M. D. Dickey, *Nat. Mater.*, 2022, **21**, 359–365.

57 J. Lee, M. W. M. Tan, K. Parida, G. Thangavel, S. A. Park, T. Park and P. S. Lee, *Adv. Mater.*, 2020, **32**, 1906679.

58 Y. Lee, W. Song and J.-Y. Sun, *Mater. Today Phys.*, 2020, **15**, 100258.

59 H. Dechiraju, M. Jia, L. Luo and M. Rolandi, *Adv. Sustainable Syst.*, 2022, **6**, 2100173.

60 Y. Bai, B. Chen, F. Xiang, J. Zhou, H. Wang and Z. Suo, *Appl. Phys. Lett.*, 2014, **105**, 151903.

61 Y. Gao, L. Shi, S. Lu, T. Zhu, X. Da, Y. Li, H. Bu, G. Gao and S. Ding, *Chem. Mater.*, 2019, **31**, 3257–3264.

62 J. Thevenin and R. Muller, *J. Electrochem. Soc.*, 1987, **134**, 273.

63 Y. Y. Lee, H. Y. Kang, S. H. Gwon, G. M. Choi, S. M. Lim, J. Y. Sun and Y. C. Joo, *Adv. Mater.*, 2016, **28**, 1636–1643.

64 Z. He and W. Yuan, *ACS Appl. Mater. Interfaces*, 2021, **13**, 1474–1485.

65 Y. Wei, H. Wang, Q. Ding, Z. Wu, H. Zhang, K. Tao, X. Xie and J. Wu, *Mater. Horiz.*, 2022, **9**, 1921–1934.

66 J. Song, S. Chen, L. Sun, Y. Guo, L. Zhang, S. Wang, H. Xuan, Q. Guan and Z. You, *Adv. Mater.*, 2020, **32**, 1906994.

67 Z. Qin, X. Sun, H. Zhang, Q. Yu, X. Wang, S. He, F. Yao and J. Li, *J. Mater. Chem. A*, 2020, **8**, 4447–4456.

68 Y. Wu, Y. Mu, Y. Luo, C. Menon, Z. Zhou, P. K. Chu and S. P. Feng, *Adv. Funct. Mater.*, 2022, **32**, 2110859.

69 X. Zhao, F. Chen, Y. Li, H. Lu, N. Zhang and M. Ma, *Nat. Commun.*, 2018, **9**, 1–8.

70 Y. Ye, Y. Zhang, Y. Chen, X. Han and F. Jiang, *Adv. Funct. Mater.*, 2020, **30**, 2003430.

71 X. Pan, Q. Wang, R. Guo, Y. Ni, K. Liu, X. Ouyang, L. Chen, L. Huang, S. Cao and M. Xie, *J. Mater. Chem. A*, 2019, **7**, 4525–4535.

72 Q. Li, J. Chen, Y. Zhang, C. Chi, G. Dong, J. Lin and Q. Chen, *ACS Appl. Mater. Interfaces*, 2021, **13**, 51546–51555.

73 I. Krossing, J. M. Slattery, C. Daguenet, P. J. Dyson, A. Oleinikova and H. Weingärtner, *J. Am. Chem. Soc.*, 2006, **128**, 13427–13434.

74 Y. Cao, Y. J. Tan, S. Li, W. W. Lee, H. Guo, Y. Cai, C. Wang and B. C.-K. Tee, *Nat. Electron.*, 2019, **2**, 75–82.

75 Y. Zhang, M. Li, B. Qin, L. Chen, Y. Liu, X. Zhang and C. Wang, *Chem. Mater.*, 2020, **32**, 6310–6317.

76 R. A. John, N. Tiwari, M. I. B. Patdillah, M. R. Kulkarni, N. Tiwari, J. Basu, S. K. Bose, C. J. Yu, A. Nirmal and S. K. Vishwanath, *Nat. Commun.*, 2020, **11**, 1–12.

77 F. Jiang, L. Ma, J. Sun, L. Guo, Z. Peng, Z. Cui, Y. Li, X. Guo and T. Zhang, *ACS Appl. Mater. Interfaces*, 2021, **13**, 14321–14326.

78 J. Lan, Y. Li, B. Yan, C. Yin, R. Ran and L.-Y. Shi, *ACS Appl. Mater. Interfaces*, 2020, **12**, 37597–37606.

79 J. I. Lee, H. Choi, S. H. Kong, S. Park, D. Park, J. S. Kim, S. H. Kwon, J. Kim, S. H. Choi and S. G. Lee, *Adv. Mater.*, 2021, **33**, 2100321.

80 P. Calvert, *Adv. Mater.*, 2009, **21**, 743–756.

81 M. L. Jin, S. Park, Y. Lee, J. H. Lee, J. Chung, J. S. Kim, J. S. Kim, S. Y. Kim, E. Jee and D. W. Kim, *Adv. Mater.*, 2017, **29**, 1605973.

82 T. Li, Y. Wang, S. Li, X. Liu and J. Sun, *Adv. Mater.*, 2020, **32**, 2002706.

83 J. Wong, A. T. Gong, P. A. Defnet, L. Meabe, B. Beauchamp, R. M. Sweet, H. Sardon, C. L. Cobb and A. Nelson, *Adv. Mater. Technol.*, 2019, **4**, 1900452.

84 M. L. Jin, S. Park, J. S. Kim, S. H. Kwon, S. Zhang, M. S. Yoo, S. Jang, H. J. Koh, S. Y. Cho and S. Y. Kim, *Adv. Mater.*, 2018, **30**, 1706851.

85 H. J. Hwang, J. S. Kim, W. Kim, H. Park, D. Bhatia, E. Jee, Y. S. Chung, D. H. Kim and D. Choi, *Adv. Energy Mater.*, 2019, **9**, 1803786.

86 N. Kim, S. Lienemann, I. Petsagkourakis, D. Alemu Mengistie, S. Kee, T. Ederth, V. Gueskine, P. Leclère, R. Lazzaroni and X. Crispin, *Nat. Commun.*, 2020, **11**, 1–10.

87 C. Chen, W. B. Ying, J. Li, Z. Kong, F. Li, H. Hu, Y. Tian, D. H. Kim, R. Zhang and J. Zhu, *Adv. Funct. Mater.*, 2022, **32**, 2106341.

88 V. Amoli, J. S. Kim, E. Jee, Y. S. Chung, S. Y. Kim, J. Koo, H. Choi, Y. Kim and D. H. Kim, *Nat. Commun.*, 2019, **10**, 1–13.

89 J. Sun, R. Li, G. Lu, Y. Yuan, X. Zhu and J. Nie, *J. Mater. Chem. C*, 2020, **8**, 8368–8373.

90 X. Xiao, M. Wang, S. Chen, Y. Zhang, H. Gu, Y. Deng, G. Yang, C. Fei, B. Chen and Y. Lin, *Sci. Adv.*, 2021, **7**, eabi8249.

91 Y. Lee, S. Lim, W. J. Song, S. Lee, S. J. Yoon, J. M. Park, M. G. Lee, Y. L. Park and J. Y. Sun, *Adv. Mater.*, 2022, 2108586.

92 Z. Cao, H. Liu and L. Jiang, *Mater. Horiz.*, 2020, **7**, 912–918.

93 Y. Xie, R. Xie, H.-C. Yang, Z. Chen, J. Hou, C. R. Lopez-Barron, N. J. Wagner and K.-Z. Gao, *ACS Appl. Mater. Interfaces*, 2018, **10**, 32435–32443.

94 J. Sun, G. Lu, J. Zhou, Y. Yuan, X. Zhu and J. Nie, *ACS Appl. Mater. Interfaces*, 2020, **12**, 14272–14279.

95 B. Yiming, X. Guo, N. Ali, N. Zhang, X. Zhang, Z. Han, Y. Lu, Z. Wu, X. Fan and Z. Jia, *Adv. Funct. Mater.*, 2021, **31**, 2102773.

96 A. Hu, C. Liu, Z. Cui, Z. Cong and J. Niu, *ACS Appl. Mater. Interfaces*, 2022, **14**, 12713–12721.

97 J. H. Kim, K. G. Cho, D. H. Cho, K. Hong and K. H. Lee, *Adv. Funct. Mater.*, 2021, **31**, 2010199.

98 Y. Zhong, G. T. Nguyen, C. D. Plesse, F. D. R. Vidal and E. W. Jager, *ACS Appl. Mater. Interfaces*, 2018, **10**, 21601–21611.

99 J. Wei, Y. Zheng and T. Chen, *Mater. Horiz.*, 2021, **8**, 2761–2770.

100 L. Xu, Z. Huang, Z. Deng, Z. Du, T. L. Sun, Z. H. Guo and K. Yue, *Adv. Mater.*, 2021, **33**, 2105306.

101 Y. Ren, J. Guo, Z. Liu, Z. Sun, Y. Wu, L. Liu and F. Yan, *Sci. Adv.*, 2019, **5**, eaax0648.

102 L. M. Zhang, Y. He, S. Cheng, H. Sheng, K. Dai, W. J. Zheng, M. X. Wang, Z. S. Chen, Y. M. Chen and Z. Suo, *Small*, 2019, **15**, 1804651.

103 J. Zhu, X. Lu, W. Zhang and X. Liu, *Macromol. Rapid Commun.*, 2020, **41**, 2000098.

104 Y. Zhang, L. Chang, P. Sun, Z. Cao, Y. Chen and H. Liu, *RSC Adv.*, 2020, **10**, 7424–7431.

105 Z. Yu and P. Wu, *Mater. Horiz.*, 2021, **8**, 2057–2064.

106 Y. Wang, S. Sun and P. Wu, *Adv. Funct. Mater.*, 2021, **31**, 2101494.

107 S. Xiang, F. Zheng, S. Chen and Q. Lu, *ACS Appl. Mater. Interfaces*, 2021, **13**, 20653–20661.

108 Z. Wang, J. Zhang, J. Liu, S. Hao, H. Song and J. Zhang, *ACS Appl. Mater. Interfaces*, 2021, **13**, 5614–5624.

109 Y. Ren, Z. Liu, G. Jin, M. Yang, Y. Shao, W. Li, Y. Wu, L. Liu and F. Yan, *Adv. Mater.*, 2021, **33**, 2008486.

110 X. Ming, C. Zhang, J. Cai, H. Zhu, Q. Zhang and S. Zhu, *ACS Appl. Mater. Interfaces*, 2021, **13**, 31102–31110.

111 B. Yiming, Y. Han, Z. Han, X. Zhang, Y. Li, W. Lian, M. Zhang, J. Yin, T. Sun and Z. Wu, *Adv. Mater.*, 2021, **33**, 2006111.

112 L. Zhang, P. Zhang, C. Chang, W. Guo, Z. H. Guo and X. Pu, *ACS Appl. Mater. Interfaces*, 2021, **13**, 46794–46802.

113 X. Zhang, L. Wang, J. Peng, P. Cao, X. Cai, J. Li and M. Zhai, *Adv. Mater. Interfaces*, 2015, **2**, 1500267.

114 X. Qu, W. Niu, R. Wang, Z. Li, Y. Guo, X. Liu and J. Sun, *Mater. Horiz.*, 2020, **7**, 2994–3004.

115 J. Lopez, D. G. Mackanic, Y. Cui and Z. Bao, *Nat. Rev. Mater.*, 2019, **4**, 312–330.

116 P. Shi, Y. Wang, K. Wan, C. Zhang and T. Liu, *Adv. Funct. Mater.*, 2022, 2112293.

117 N. Angulakshmi, R. S. Kumar, M. A. Kulandainathan and A. M. Stephan, *J. Phys. Chem. C*, 2014, **118**, 24240–24247.

118 C. Zhang, H. Zheng, J. Sun, Y. Zhou, W. Xu, Y. Dai, J. Mo and Z. Wang, *Adv. Mater.*, 2021, 2105996.

119 R. Li, T. Fan, G. Chen, K. Zhang, B. Su, J. Tian and M. He, *Chem. Mater.*, 2020, **32**, 874–881.

120 J. D. Mota-Morales, R. J. Sánchez-Leija, A. Carranza, J. A. Pojman, F. del Monte and G. Luna-Bárcenas, *Prog. Polym. Sci.*, 2018, **78**, 139–153.

121 T. Fan, G. Chen, H. Xie, B. Su and M. He, *Chem. Eng. J.*, 2020, **393**, 124685.

122 P. Sang, R. Li, K. Zhang, G. Chen, K. Zhao and M. He, *ACS Appl. Polym. Mater.*, 2022, **4**(5), 3543–3551.

123 K. Zhang, G. Chen, J. Yang, J. Tian and M. He, *J. Mater. Chem. A*, 2021, **9**, 4890–4897.

124 C. Dang, M. Wang, J. Yu, Y. Chen, S. Zhou, X. Feng, D. Liu and H. Qi, *Adv. Funct. Mater.*, 2019, **29**, 1902467.

125 X. Li, J. Liu, Q. Guo, X. Zhang and M. Tian, *Small*, 2022, 2201012.

126 W. Zhang, B. Wu, S. Sun and P. Wu, *Nat. Commun.*, 2021, **12**, 1–12.

127 Z. Lei and P. Wu, *Nat. Commun.*, 2019, **10**, 1–9.

128 T. Long, Y. Li, X. Fang and J. Sun, *Adv. Funct. Mater.*, 2018, **28**, 1804416.

129 Z. Lei and P. Wu, *Mater. Horiz.*, 2019, **6**, 538–545.

130 D. Dong, C. Tsao, H.-C. Hung, F. Yao, C. Tang, L. Niu, J. Ma, J. MacArthur, A. Sinclair and K. Wu, *Sci. Adv.*, 2021, **7**, eabc5442.

131 D. Pei, S. Yu, X. Zhang, Y. Chen, M. Li and C. Li, *Chem. Eng. J.*, 2022, 136741.

132 H. Ohno, M. Yoshizawa-Fujita and Y. Kohno, *Phys. Chem. Chem. Phys.*, 2018, **20**, 10978–10991.

133 C. Ohm, M. Brehmer and R. Zentel, *Adv. Mater.*, 2010, **22**, 3366–3387.

134 K. M. Herbert, H. E. Fowler, J. M. McCracken, K. R. Schlafmann, J. A. Koch and T. J. White, *Nat. Rev. Mater.*, 2021, 1–16.

135 T. Kato, Y. Hirai, S. Nakaso and M. Moriyama, *Chem. Soc. Rev.*, 2007, **36**, 1857–1867.

136 Y. Wang, Y. Chen, J. Gao, H. G. Yoon, L. Jin, M. Forsyth, T. J. Dingemans and L. A. Madsen, *Adv. Mater.*, 2016, **28**, 2571–2578.

137 M. Yao, B. Wu, X. Feng, S. Sun and P. Wu, *Adv. Mater.*, 2021, **33**, 2103755.

138 F. Wang, P. Altschuh, L. Ratke, H. Zhang, M. Selzer and B. Nestler, *Adv. Mater.*, 2019, **31**, 1806733.

139 M. W. Schulze, L. D. McIntosh, M. A. Hillmyer and T. P. Lodge, *Nano Lett.*, 2014, **14**, 122–126.

140 M. J. Lee, J. Han, K. Lee, Y. J. Lee, B. G. Kim, K.-N. Jung, B. J. Kim and S. W. Lee, *Nature*, 2022, **601**, 217–222.

141 B. I. Shklovskii and A. L. Efros, *Electronic properties of doped semiconductors*, Springer Science & Business Media, 2013.

142 B. Lovrecek, A. Despic and J. Bockris, *J. Phys. Chem.*, 1959, **63**, 750–751.

143 Z. Gadjourova, Y. G. Andreev, D. P. Tunstall and P. G. Bruce, *Nature*, 2001, **412**, 520–523.

144 L. Krasemann and B. Tieke, *Langmuir*, 2000, **16**, 287–290.

145 O. J. Cayre, S. T. Chang and O. D. Velev, *J. Am. Chem. Soc.*, 2007, **129**, 10801–10806.

146 R. Skouri, F. Schossele, J. Munch and S. Candau, *Macromolecules*, 1995, **28**, 197–210.

147 I. Vlassioulk, T. R. Kozel and Z. S. Siwy, *J. Am. Chem. Soc.*, 2009, **131**, 8211–8220.

148 J. H. Han, K. B. Kim, H. C. Kim and T. D. Chung, *Angew. Chem., Int. Ed.*, 2009, **48**, 3830–3833.

149 K. Tybrandt, R. Forchheimer and M. Berggren, *Nat. Commun.*, 2012, **3**, 1–6.

150 K. Tybrandt, K. C. Larsson, A. Richter-Dahlfors and M. Berggren, *Proc. Natl. Acad. Sci. U. S. A.*, 2010, **107**, 9929–9932.

151 A. Guha, T. J. Kalkus, T. B. Schroeder, O. G. Willis, C. Rader, A. Ianiro and M. Mayer, *Adv. Mater.*, 2021, **33**, 2101757.

152 H. Wang, Y. Sun, T. He, Y. Huang, H. Cheng, C. Li, D. Xie, P. Yang, Y. Zhang and L. Qu, *Nat. Nanotechnol.*, 2021, **16**, 811–819.

153 S. I. Sadovnikov, *Russ. Chem. Rev.*, 2019, **88**, 571.

154 M. Bredol and H. Schulze Dieckhoff, *Materials*, 2010, **3**, 1353–1374.

155 C. H. Yang, B. Chen, J. Zhou, Y. M. Chen and Z. Suo, *Adv. Mater.*, 2016, **28**, 4480–4484.

156 J. Wang, C. Yan, G. Cai, M. Cui, A. Lee-Sie Eh and P. See Lee, *Adv. Mater.*, 2016, **28**, 4490–4496.

157 F. Stauffer and K. Tybrandt, *Adv. Mater.*, 2016, **28**, 7200–7203.

158 S. H. Cho, S. W. Lee, I. Hwang, J. S. Kim, B. Jeong, H. S. Kang, E. H. Kim, K. L. Kim, C. Park and C. Park, *Adv. Opt. Mater.*, 2019, **7**, 1801283.

159 L. Shi, C. Zhang, Y. Du, H. Zhu, Q. Zhang and S. Zhu, *Adv. Funct. Mater.*, 2021, **31**, 2007863.

160 Y. Zhou, S. Cao, J. Wang, H. Zhu, J. Wang, S. Yang, X. Wang and D. Kong, *ACS Appl. Mater. Interfaces*, 2018, **10**, 44760–44767.

161 Y. Zhou, C. Zhao, J. Wang, Y. Li, C. Li, H. Zhu, S. Feng, S. Cao and D. Kong, *ACS Mater. Lett.*, 2019, **1**, 511–518.

162 Y. J. Tan, H. Godaba, G. Chen, S. T. M. Tan, G. Wan, G. Li, P. M. Lee, Y. Cai, S. Li and R. F. Shepherd, *Nat. Mater.*, 2020, **19**, 182–188.

163 B. Jiang, J. Iocozzia, L. Zhao, H. Zhang, Y.-W. Harn, Y. Chen and Z. Lin, *Chem. Soc. Rev.*, 2019, **48**, 1194–1228.

164 R. P. Ortiz, A. Facchetti and T. J. Marks, *Chem. Rev.*, 2010, **110**, 205–239.

165 L. J. Romasanta, M. A. López-Manchado and R. Verdejo, *Prog. Polym. Sci.*, 2015, **51**, 188–211.

166 C. A. Kraus, *J. Phys. Chem.*, 1956, **60**, 129–141.

167 J.-M. Park, J. Park, Y.-H. Kim, H. Zhou, Y. Lee, S. H. Jo, J. Ma, T.-W. Lee and J.-Y. Sun, *Nat. Commun.*, 2020, **11**, 1–10.

168 Y. Liu, T. Chen, Z. Jin, M. Li, D. Zhang, L. Duan, Z. Zhao and C. Wang, *Nat. Commun.*, 2022, **13**, 1–11.

169 M. V. Kovalenko, L. Protesescu and M. I. Bodnarchuk, *Science*, 2017, **358**, 745–750.

170 Q. Zhou, Z. Bai, W. G. Lu, Y. Wang, B. Zou and H. Zhong, *Adv. Mater.*, 2016, **28**, 9163–9168.

171 Y. Wang, J. He, H. Chen, J. Chen, R. Zhu, P. Ma, A. Towers, Y. Lin, A. J. Gesquiere and S. T. Wu, *Adv. Mater.*, 2016, **28**, 10710–10717.

172 Y. Zhang, Y. Zhao, D. Wu, J. Xue, Y. Qiu, M. Liao, Q. Pei, M. S. Goorsky and X. He, *Adv. Mater.*, 2019, **31**, 1902928.

173 Y. Xin, H. Zhao and J. Zhang, *ACS Appl. Mater. Interfaces*, 2018, **10**, 4971–4980.